SCIENCE CHINA
Earth Sciences

•REVIEW•

https://doi.org/10.1007/s11430-022-1085-y

Volcanism in the Solar System

Long XIAO[1*], Jun HUANG[1], Zhiyong XIAO[2], Chao QI[3,4] & Yuqi QIAN[1]

[1] *School of Earth Sciences, China University of Geosciences, Wuhan 430074, China;*
[2] *School of Atmospheric Sciences, Sun Yat-sen University, Zhuhai 519082, China;*
[3] *Key Laboratory of Earth and Planetary Physics, Institute of Geology and Geophysics, Chinese Academy of Sciences, Beijing 100029, China;*
[4] *College of Earth and Planetary Sciences, University of Chinese Academy of Sciences, Beijing 100049, China*

Received April 30, 2022; revised January 28, 2023; accepted February 28, 2023; published online August 14, 2023

Abstract Volcanic activity is the main process for heat-material exchange and circulation for differentiated planets. All terrestrial planets in the Solar System, the Moon, the satellites of giant planets, and the dwarf planets once experienced or are currently experiencing volcanic activities. This paper summarized the volcanism (main volcanic features and their formation) on the Moon, Mars, Venus, and Mercury in the inner Solar System, volcanism and cryovolcanism on satellites (Io, Europa, Enceladus) of giant planets, as well as volcanism on dwarf planets including Cere in the main asteroid belt and Pluto in the Kuiper belt. This work shows volcanism in the Solar System is driven by various factors, forming abundant volcanic landforms. It has significant meanings to compare volcanism happening on different planets using comparative planetology approaches for a better understanding of volcanism, the planetary habitability, and the information contained on the origin and evolution of planets in the Solar System.

Keywords Volcanism, Terrestrial planets, Planetary evolution, Solar System

Citation: Xiao L, Huang J, Xiao Z, Qi C, Qian Y. 2023. Volcanism in the Solar System. Science China Earth Sciences, 66, https://doi.org/10.1007/s11430-022-1085-y

1. Introduction

Volcanism is the phenomenon that solid, liquid, gas, and their mixtures erupt to the surface during the thermal evolution process of planets, satellites, and asteroids. The planet bodies in the Solar System have various eruption styles and products. Except for the silicate melt erupted from the Earth, ultramafic and sulfur-rich melts erupted from Io, and water ice and alkane melts erupted from icy moons in the outer Solar System and dwarf planets. All volcanic activities were controlled by two factors, i.e., heat source and melted materials.

According to the study of terrestrial volcanology, present volcanic activities on the Earth are mainly controlled by plate tectonics and mantle plume. Mantle convection and long half-life period radioactive elements ^{40}K, ^{235}U, and ^{238}Th are the main heat source for terrestrial volcanism. However, in the planetesimal formation stage, remnant planetesimals keeping aggregation, the heat converted from kinetic energy and the short half-life period radioactive element ^{26}Al are significant. With the growth of the planet's body, self-compaction may raise the temperature of the interior of a planet (Francis and Oppenheimer, 2004). This heat is likely to be the main heat source for the melting of relatively large asteroids such as Ceres. For the even larger differentiated planet, the formation of the core provides a continuous heat source for the volcanism (Solomon et al., 1981).

The tidal energy from planet movement is another important heat source. For the Earth-Moon system, gravitation triggers prominent liquid tides, but not enough to change the internal thermal state of the Earth. Venus does not have a satellite; the two satellites of Mars are too small. Therefore,

* Corresponding author (email: longxiao@cug.edu.cn)

both of them have little to no tidal heat. Mercury is very close to the Sun; orbit resonance may impact its internal thermal state, but could not support the current volcanism. However, for moons in the outer Solar System, such as Io, Europa, and Enceladus, the tidal heat may be the main heat source for volcanism or cryovolcanism (Wilson, 2009). For dwarf planets like Pluto, the heat source for its cryovolcanism is still not unclear.

Since the formation of planets, the heat from interior radioactive decay is decreasing and the surface heat flux is decreasing as well in a continuous process of cooling. Current studies show most planets obey the general thermal evolution trend of a planet, but the discrepancy between model prediction and observations prompts scientists to rethink the heat source, eruption mechanism, the diversity of volcanic products, and the evolution of volcanism in different bodies in the Solar System. This paper is aimed to summarize the volcanism on the main planets in the Solar System first, on the basis of which propose key scientific questions of planetary volcanism and future exploration targets.

2. Volcanism in the inner Solar System

Earth is the most familiar planet to humans. It is also the reference object to other planets when studying their volcanic activities. Here we focus mainly on discussing the recent advancement of volcanism on the Moon, Mars, Venus, and Mercury.

2.1 Volcanism on the Moon

Moon is the only natural satellite of the Earth with an average distance to the Earth of 384,400 km, which has a diameter of 1,737.4 km, a bulk density of 3.344 g cm^{-3}, and a surface gravitational acceleration of 1.624 m s^{-2}. The Moon formed at ~4.5 Ga (Yin et al., 2002; Kleine et al., 2002; Barboni et al., 2017) by the impact of a Mars-sized planetary body, Theia, and the proto-Earth (Halliday, 2000). The giant impact melted the entire lunar surface to form the lunar magma ocean (Warren, 1985). The lunar volcanism started at the end of the solidification of the lunar magma ocean (~4.35 Ga; Terada et al., 2007), and lasted until at least 2.0 Ga ago (Che et al., 2021; Li et al., 2021), even 1.2 Ga ago (Hiesinger et al., 2011; Qian et al., 2023). Lunar volcanism is the most important endogenic geological process and is a skylight to probe the internal properties and thermal evolution of the Moon.

Lunar basalts are the most significant products of lunar volcanism. Mare and cryptomare occupy at least 18% area of the lunar surface (Whitten and Head, 2015a), with a total volume of 1×10^7 km^3, reaching 1% volume of the whole lunar crust. The majority of mare basalts distribute within the large impact basins, especially those formed in and after the Nectarian Period, such as Imbrium basin, Serenitatis basin, Tranquillitatis basin, Nectaris basin, and Crisium basin, forming widespread lava plains (Qiao et al., 2021). The nearside and farside of the Moon have a prominent dichotomy, characterized by asymmetrical crustal thickness, elevation, geological and thermal history (Laneuville et al., 2013). Most of the lunar basalts develop in the lunar nearside, only a few in the farside and limited to the South Pole-Aitken basin, Orientale basin, and a few other large basins. The Procellarum KREEP Terrane (Jolliff et al., 2000) in the lunar nearside has most of the lunar basalts (Hiesinger et al., 2011). Three huge volcanic complexes, Mons Rümker, Aristarchus Plateau, and Marius Hills are located to the north, middle, and south of Procellarum KREEP Terrane, becoming the most prominent features on the Moon (Figure 1). In addition, all young lunar volcanism happened within the Procellarum KREEP Terrane, concentering at the center of Oceanus Procellarum and the southwest of Mare Imbrium. It may be due to the enrichment of the heat-producing elements and the thin crust within the Procellarum KREEP Terrane (Laneuville et al., 2013), but Chang'e-5 samples have yet to test this hypothesis.

Lunar volcanism includes effusive and explosive eruptions. The effusive eruption is controlled by eruption rate, eruption duration, cooling rate, magma supply, and topography, to form various volcanic features (Head and Wilson, 2017; Zhang et al., 2017). Low eruption flux and quick cooling rate tend to form small shield volcanoes; high eruption flux and quick cooling rate tend to form compound lava flow; high-flux and long-duration eruption accelerates thermal erosion and tend to form sinuous rilles; even higher flux may produce huge lava flows with a length of hundreds of kilometers. Because of the difference in eruption conditions, explosive eruption also includes different styles (Head and Wilson, 2017). The strombolian eruption could form cinder and spatter cones; the Hawaiian eruption could form pyroclastic blankets; the Ultraplinian eruption could cause Moon-wide dispersal of gas and foam droplets; the Vulcanian eruption could form dark-halo craters mixing with country rocks; the Ionian eruption could form dark pyroclastic rings, multiple eruptions from many gas-rich fissures could create dark mantles; long-duration high-effusion rate eruptions accompanied by continuing pyroclastic activity could cause a central thermally eroded lava pond and channel. In addition, underplating and silicate liquid immiscibility may produce silicic magma, whose eruption consists of silica-rich volcanoes, including those distributed in Gruithuisen, Aristarchus, Hansteen, Riphaeus, Lassell, and Helmet regions (Figure 2).

Recently, several types of special volcanic landforms on the Moon were found or re-recognized. Irregular mare patch

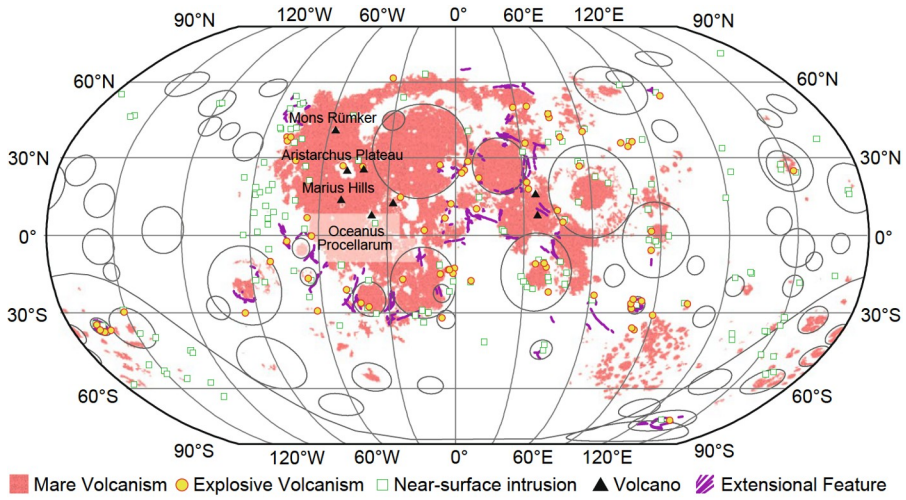

Figure 1 Distribution of lunar volcanic features. This figure is modified from Byrne (2020), Copyright © 2019 Springer Nature.

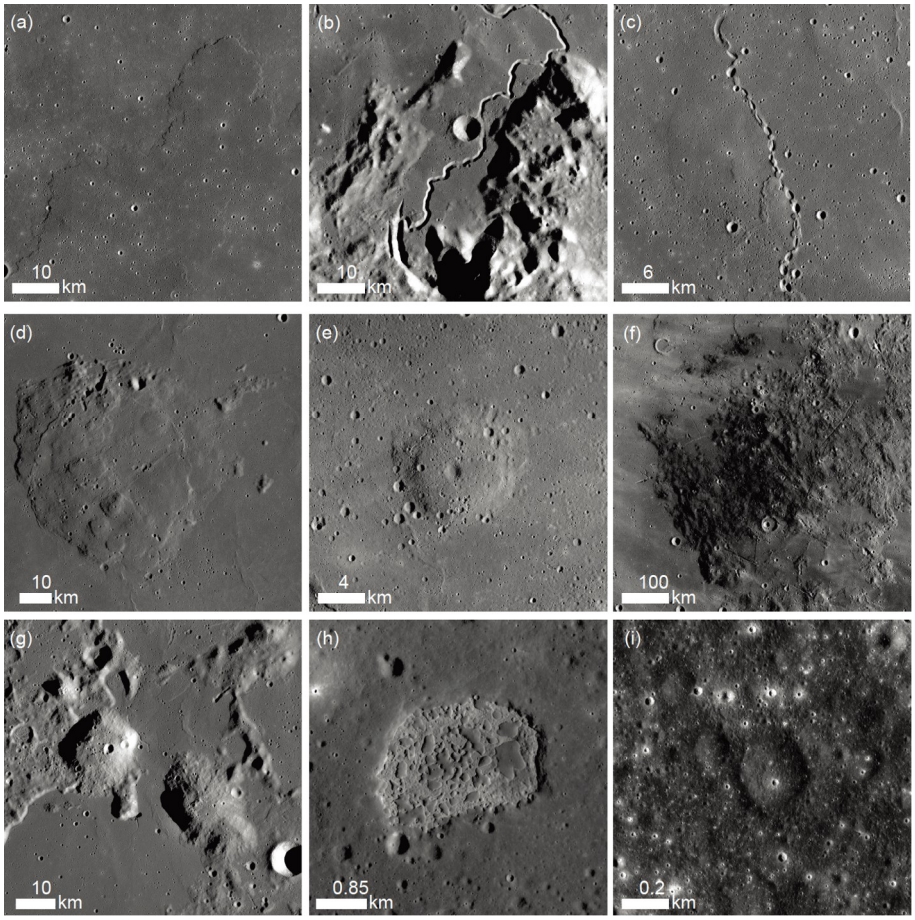

Figure 2 Typical lunar volcanic features. (a) Lava flows in the center of Mare Imbrium (22.45°W, 31.95°N); (b) Hadley Rille in the southeast of Mare Imbrium (2.74°E, 25.35°N); (c) lava tube to the northwest of Gruithuisen domes (43.479°W, 34.583°N); (d) Mons Rümker (57.9°W, 40.70°N); (e) dome to the west of Milichius crater (31.24°W, 10.09°N); (f) pyroclastic deposits to the northwest of Schröter crater (7.90°W, 5.91°N); (g) Gruithuisen domes (40.14° W, 36.43°N); (h) irregular mare patch Ina (5.30°E, 18.15°N); (i) Ring moat dome structure in the center of Mare Tranquillitatis. The basemaps of (a)–(g) are the Kaguya TC Morning Map. The basemaps of (h) and (i) are LROC NAC images. North is up for all figures.

is characterized by its unique irregular appearance, with well-preserved subtle topography fluctuation, low optical maturity, and few overlaying craters (Qiao et al., 2017). So far, there are 91 irregular mare patches discovered, mainly in

the mare region in the lunar nearside (Qiao et al., 2020). The origin of the irregular mare patch still remains controversial. Braden et al. (2014) propose the irregular mare patch as the product of young volcanism within 100 Ma. Qiao et al. (2017) and Head and Wilson (2017) suggest they are formed by ancient lava lake processes before 3.0 Ga, accompany by magmatic foam extrusions. Ring-moat dome structure is a newly discovered morphological feature widespread on the lunar basaltic lava flows; these low domes are typically surrounded by narrow annular depressions or moats (Zhang et al., 2017). So far, there are more than 8000 ring-moat dome structures discovered, mainly distributed in the lava plains within Mare Tranquillitatis, Mare Fecunditatis, Oceanus Procellarum, Mare Humorum, Mare Nubium, and Mare Imbrium (Zhang et al., 2020). The formation of the ring-moat dome structure is also in controversy. Zhang et al. (2017) and Wilson et al. (2019) proposed they are formed by magmatic foam extrusions. Flow inflation and the formation of the foam layers fracture the upper crustal layer that permits extrusions of the magmatic foams to form domes, with subsidence of the adjacent surface to form the moats. Garrick-Bethell and Seritan (2021) suggested the origin of ring-moat dome structures is related to the shallow magma intrusion and sill formation. Fitz-Gerald (2021) thought the ring-moat dome structure is formed by the spherical aggregation of lunar regolith driven by the moonquake, but this hypothesis lacks geophysical evidence. The formation time of ring-moat dome structures is also unclear; Zhang et al. (2021) found several of them may form as recently as 100 Ma.

Latest lunar missions, such as the Chang'e-5 mission (Zhou et al., 2022), significantly promote the development of lunar volcanology. Chang'e-5 landed in an Eratosthenian-aged mare unit in the northern Oceanus Procellarum, ~170 km away from Mons Rümker (Qian et al., 2021). The returned Chang'e-5 samples indicate the mare basalts in this region have an age of ~2.0 Ga (Che et al., 2021; Li et al., 2021), at least 800 Ma younger than the previous estimation of the end of lunar volcanism (Liu et al., 2021). The analysis of U-Pb, Rb-Sr, and H isotopes and trace elements indicate that the mantle source of Chang'e-5 basalts is not rich in heat-producing elements (Tian et al., 2021) or water (Hu et al., 2021), challenging the current lunar thermal evolution model (Liu et al., 2021; Mitchell, 2021). Although Chang'e-5 returned young lunar basalts, more young samples are needed to be returned, including those from irregular mare patches and ring-moat dome structures, in order to fully understand the young lunar volcanism.

2.2 Volcanism on Mercury

As the inner-most planet in the Solar System, Mercury has a comparable diameter (~2440 km) with the Earth's Moon and a comparable surface gravity with Mars. With a large iron-rich core, Mercury is the only terrestrial body besides the Earth that has a dipole magnetic field, which is much weaker but highly dynamic. There is no convectional atmosphere on Mercury, and the powerful solar wind at the orbital position of Mercury exhibits rich interactions with the magnetosphere and surface materials. In general, the space environment and surface morphology of Mercury is rather similar to those on the Moon.

Mercury and other terrestrial bodies share similarities in terms of the evolution of volcanism. The hypothesized primary crust of Mercury, which was likely differentiated from a postulated magma ocean, has been largely buried by later volcanic materials, which were then substantially mixed by impact bombardment. On the other hand, the lithology of igneous rocks, volcanic landforms, eruption mechanism, and durations on Mercury exhibit important differences from those on the other terrestrial bodies. Surface materials on Mercury contain <2 wt% of iron and 0.4 wt% of Ti, which are much lower than the global average of lunar surface materials (Weider et al., 2016). However, the contents of Mg (9–25 wt%) and S (~4 wt%) on Mercury are substantially larger than those of other terrestrial bodies (McCoy et al., 2018). Igneous rocks on Mercury are likely mainly alkaline-rich komatiite and boninite (Vander Kaaden et al., 2017; McCoy et al., 2018), which are composed of felspar, pyroxene, and olivine, while minor contents of quartz may also exist (Charlier et al., 2013; Vander Kaaden et al., 2017). The viscosity of magma formed in Mercury is rather low (0.4–82 Pa s; McCoy et al., 2018), and the mobility of Mercurian magma is much larger than that on the other terrestrial bodies (Stockstill-Cahill et al., 2012; Byrne et al., 2018). Therefore, with sufficiently-large eruption flux, volcanism on Mercury can easily form large lava plains similar to large igneous provinces on Earth and the other terrestrial bodies.

Intercrater plains (Trask and Guest, 1975) and smooth plains (Denevi et al., 2013) are the major volcanic landforms on Mercury in terms of volume (Figure 3a). Intercrater plains, by definition, are composed of plain materials that have buried numerous impact structures, which can be as large as ~128 km (Figure 3b, 3c). The voluminous flooding event that formed intercrater plains substantially reduced the spatial density of impact craters at the diameter range of 20–128 km (Fassett et al., 2011). Stratigraphic relationships between intercrater plains and the other terranes on Mercury suggest that intercrater plains were formed early in history, mostly larger than ~4.1 Ga. However, there has been a long debate about the possible cause of the flooding event that formed intercrater plains, since they can be explained by both effusive volcanism and/or deposition of melt-rich ejecta deposits from large impact basins (Spudis and Guest, 1988; Strom et al., 2011). Recent observations based on multi-band

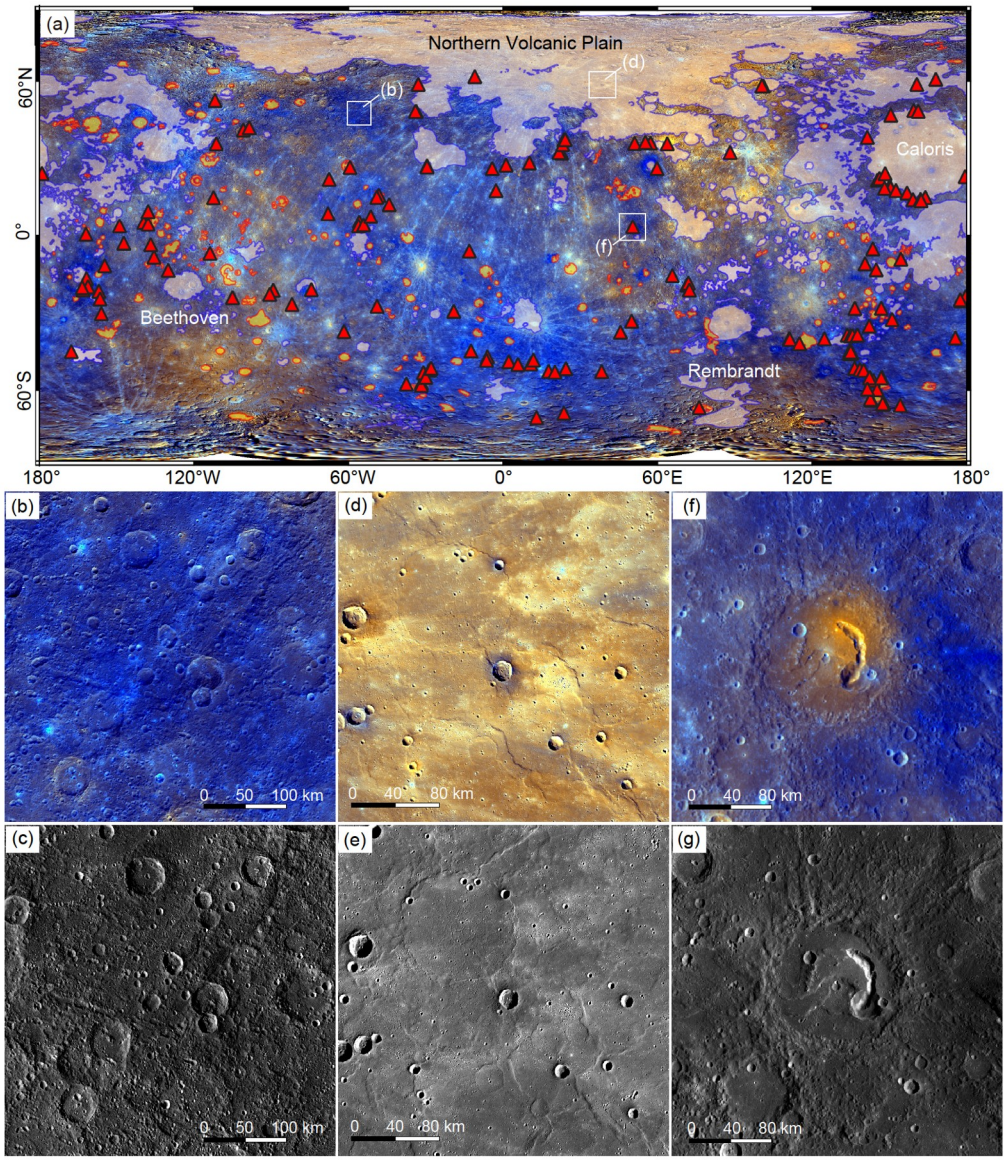

Figure 3 Volcanic plains and pyroclastic deposits on Mercury. (a) Smooth plains with various origins (pink shades with blue margins are confirmed volcanic plains, yellow shades with red margins are suspicious volcanic plains that need more evidence) and pyroclastic deposits (red triangles). The base image is the enhanced color mosaic obtained by the MESSENGER spacecraft. (b), (c), Intercrater plains; (d), (e), smooth plains; (f), (g), volcanic pits and their surrounding pyroclastic deposits.

images that were returned by the MESSENGER spacecraft showed that intercrater plains exhibit similar reflectance spectra and geochemical characteristics with typical lava flows and lava plains on Mercury (Whitten et al., 2014; Murchie et al., 2018). Meanwhile, ejecta deposits formed by known impact basins on Mercury are much smaller than the volume of intercrater plains on Mercury, further suggesting that most intercrater plains may be formed by early effusive volcanism. The spatial density of large impact craters on the most-heavily cratered terrains is comparable with that of major impact basins on Mercury, indicating that Mercury might have experienced a global volcanic resurfacing that has removed earlier geological history at ~4.1 Ga (Marchi et al., 2013).

Smooth plains are composed of high-reflectance, flat plain materials that filled low elevation areas on Mercury (Denevi et al., 2013; Figure 3a). Surface areas of individual smooth plains are from 10^2 to 10^6 km^2 (Byrne et al., 2016; Wang et al., 2021), and thicknesses of over several kilometers. Smooth plains mainly occur in areas with thin crust thicknesses (Wang et al., 2021), typically in floors of large impact craters. Smooth plains cover ~27% of the global surface, and they have a smaller density of impact craters than the other major terranes on Mercury. Meanwhile, it is noticed that the temporal-spatial distributions of smooth plains on Mercury exhibit a close correlation with major impact basins such as

the Caloris, Rembrandt, and Beethoven basins, and these basins were formed around ~3.8 Ga (Whitten and Head, 2015b; Mancinelli et al., 2016; Byrne et al., 2018). Smooth plains are located around these large impact basins, while in the antipodal regions of the basins, smooth plains do not show obvious concentrations (Wang et al., 2021). Absolute model ages for smooth plains were derived based on crater statistics, yielding a rather uniform age of ~3.6–3.8 Ga, i.e., within 200 million years around 3.7 Ga (Wang et al., 2021). Therefore, the formation of most smooth plains on Mercury may be spatially and temporally correlated with the formation of the large impact basins, since a single basin-forming impact could induce thermal disturb in the mantle of Mercury for over 100 Myr (Padovan et al., 2017). The concentrated formation of large impact basins might have ingested substantial energy in the interior of Mercury, forming widespread giant faults in the lithosphere and promoting the degree of partial melting in the mantle. Therefore, the last global volcanic resurfacing event on Mercury might also be triggered by the basin forming events.

Over 170 locations of high-reflectance and reddish pyroclastic deposits exist on Mercury, and they occur around irregularly-shaped and rimless depressions (Figure 3f, 3g). Pyroclastic deposits on Mercury are much larger in size than those on the Moon, although Mercury has a larger surface gravity (Besse et al., 2020). Therefore, the magma that drove the explosive eruptions on Mercury contains a substantially higher content of volatiles, and the eruption speed is much larger (Kerber et al., 2009; Thomas et al., 2015). One of the largest pyroclastic deposits on Mercury, the Nathair Facular, contain less amounts of S (Weider et al., 2016; Peplowski et al., 2016) than the surrounding terranes, suggesting that oxides of C and S might be the volatiles that drove the explosive eruptions. Besides brightish pyroclastic deposits, darkish pyroclastic deposits are recently observed on Mercury, and some of them were formed in the Kuiperian (Xiao et al., 2021). Such darkish pyroclastic deposits exhibit weak absorption features at about 600 nm, indicating existence of graphite (Figure 4d~4f). Most pyroclastic deposits occur around pre-existing crustal weaknesses, such as impact structures, tectonic features, and older volcanoes (Goudge et al., 2014; Jozwiak et al., 2018). Regional concentrations of pyroclastic deposits also occur in certain regions, such as the circumferential Caloris region (Figure 3a). The morphology and geometry of the pyroclastic deposits suggest that they were formed by Vulcanian-type eruptions (Besse et al., 2020). Detection of graphite in the darkish pyroclastic deposits suggests that carbon might not be completely exhausted from the magma during partial melting or ascending, or that the explosive eruptions have fractured and dispersed the cap rocks, which were rich in graphite, to form the pyroclastic deposits (Weider et al., 2016; Xiao et al., 2021). Overpressure of volatiles in the ascending magma, especially in the magma chamber phases, would overcome the burden pressure of the country rocks, forming the explosive eruptions.

Volcanic activity on Mercury mainly occurred in the first 1 billion years after the formation of the planet, when the interior of Mercury was much hotter due to strong heating by short-period radiometric elements and impact bombardment (Deng et al., 2020). Therefore, at least two near-global resurfacing events occurred, forming the global distributions of intercrater plains and smooth plains. The geophysical model for the thermal evolution of Mercury predicted that the planet entered the stage of net compression since ~3.8 Ga. The dominating compressive stress in the lithosphere of Mercury reduces the possibility of magma ascending to the surface afterward. Meanwhile, the substantially cooled interior and reduced production efficiency of heat also lowered the amount of partial melting in the mantle. Therefore, since ~3.5 Ga, effusive volcanism has basically stopped on Mercury, and flooding lava could only ascend to the surface at locations with extremely thin crusts (Wang et al., 2021). On the other hand, explosive eruptions that formed pyroclastic deposits have continued in geological recent times (Thomas et al., 2014; Xiao et al., 2021). With the dominating compressional stress of the lithosphere and a reduced heat production rate in the mantle, the magma in Mercury may contain a high content of volatiles, which could drive rapid ascending to the surface.

In the catalog of meteorites discovered on Earth, no confirmed samples were sourced from the planet Mercury. The sample-return mission has not been performed on Mercury either. Therefore, the basic geochemical characteristics of Mercury, which are deduced from remote observations, lack calibration from sample analyses. Current observations suggest that element abundances on Mercury are not strictly correlated with surface reflectances. Meanwhile, spatial resolutions of element detection are usually much coarser than the mapping of reflectance, so the element contents of different color units are not well known. Meanwhile, petrological modeling revealed that due to the low content of iron and low oxygen fugacity of the mantle, magma formed in Mercury has a substantially low density, so intrusive bodies might be minor in the lithosphere. However, available geophysical data (e.g., gravity data) are not adequate in the spatial resolution to detect possible intrusive plutons, which also prohibits investigating the mechanism of magma ascending in the interior.

The ESA-JAXA joint Mercury spacecraft, Bepi-Colombo is currently on the way to the planet Mercury, which will be inserted into orbit around Mercury in 2025. Detections by this spacecraft would substantially improve the information dimensions and spatial resolutions of data for the space environment, interior structures, and surface physical and chemical characteristics of Mercury. The upcoming new

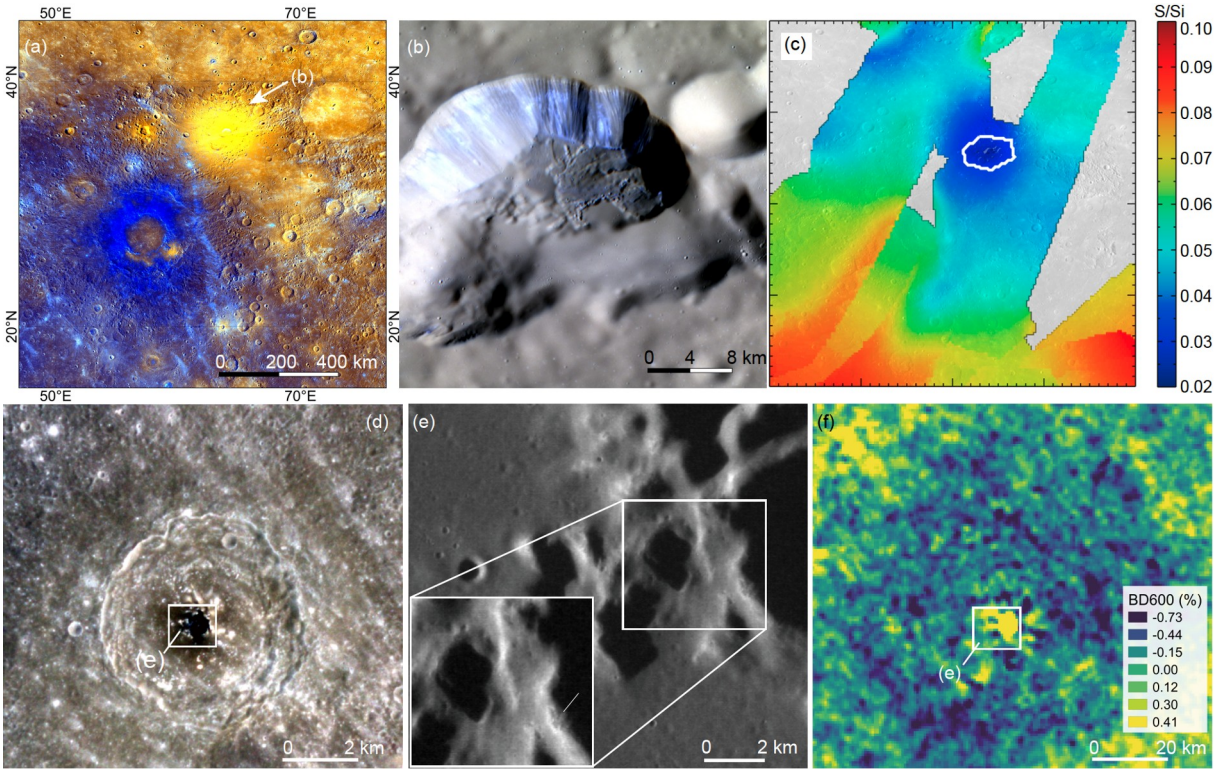

Figure 4 High-reflectance and low-reflectance pyroclastic deposits on Mercury. (a) The Nathair Facular on Mercury; (b) central volcanic pit in the Nathair Facular; (c) content of S/Si in the Nathair Facular (Weider et al., 2016), Copyright © 2016 American Geophysical Union; (d) a darkish pyroclastic deposit in the center of an unnamed crater (centered at 155.8°E, 4.7°N); (e) volcanic pit in the pyroclastic deposit; (f) absorption depths of graphite in the darkish pyroclastic deposits. (d)–(e) from Xiao et al. (2021), Copyright © 2021 American Geophysical Union.

generation of scientific data would substantially improve our understanding of the planet Mercury. Furthermore, while mission concepts of sample return from Mercury have been proposed for decades, recent years saw the fast movements of such demonstrations. Sample return from Mercury and identification of mercurian meteorites on Earth are crucial to improve our understanding of the geochemistry of this planet.

2.3 Volcanism on Venus

Venus is the second planet in the inner Solar System, with lots of similarities to the Earth. Venus has a diameter of 12,103 km, with an average distance to the Sun of 0.7 AU, a bulk density of 5.243 g cm^{-3}, and a surface gravitational acceleration of 8.87 m s^{-2}. Venus has a dense atmosphere with a surface pressure intensity of 92 bar, consisting of CO_2 (96.5%) and N_2 (3.5%). The greenhouse effect is strengthened by the dense atmosphere, making Venus has an average temperature of 464°C. In addition, the dense atmosphere and the hot surface of Venus significantly affected its volcanic activities.

Venus does not have plate tectonics, the dense atmosphere reduces the influence of the impact process on the surface of Venus; therefore, volcanism becomes the main driving force to alter the surface of Venus (Nimmo and McKenzie, 1998; Strom et al., 1994). Impact crater countings indicate the surface of Venus has a surface age of 300 Ma–1.0 Ga, representing the age of the surface volcanic deposits. Recent research even suggests the volcanism of Venus may last until the present (Smrekar et al., 2010; Filiberto et al., 2020). The volcanism of Venus is very active, whose products overlap with pre-existing volcanic deposits, making it hard to study the volcanism formed in the early stage.

The scale of volcanic landforms varies a lot on Venus (Figure 5). The volcanic landforms on Venus include volcanic centers (such as large volcanoes, intermediate volcanoes, small volcanoes, and calderas as well as special features like coronas, arachnoids, and novae) and lava flow-style features (such as lava flow and lava channel).

Large volcanoes are volcanic centers with a diameter larger than 100 km; there are around 156 large volcanoes discovered on Venus. Large volcanoes are characterized by radial lava flows, in companies with concentric and circular features, developing in high-elevation and structural convergence regions. Some large volcanoes have apparent craters on the top. Representative large volcanoes include Sif and Gula in the west of Eistla region. Intermediate volcanoes have diameters between 20 and 100 km. They usually have symmetrical shield shapes depicted by radial lava flows or fractures. According to the morphology of intermediate volcanoes, they are further subdivided into simple-shaped,

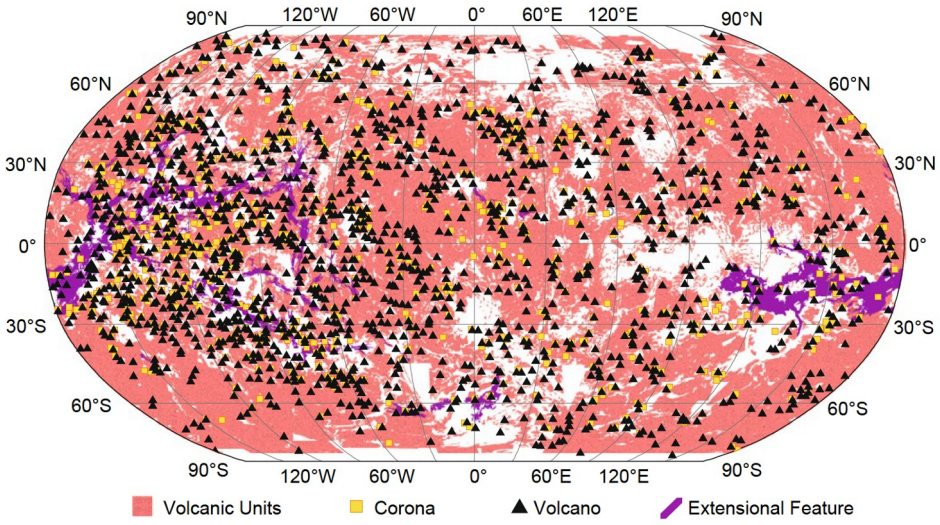

Figure 5 Distribution of volcanic features and units on Venus. This figure is modified from Byrne (2020), Copyright © 2019 Springer Nature.

anemone-shaped, pancake-shaped, and tick-shaped volcanoes. Small volcanoes smaller than 20 km are most widely spread on Venus, tending to gather together to form volcanic clusters. There are around 10,000 small volcanoes and 566 volcanic clusters discovered on Venus (Head et al., 1992). Small volcanoes have round or elliptic shapes with gentle slopes. In addition, coronae are unique volcanic features on Venus, with a total number of 362. Coronae could be further classified into concentric, concentric-double ring, asymmetric, radial/concentric, and multiple classes coronae on the basis of their morphologies (Stofan et al., 1992). The sizes of coronae vary from 60 to 2000 km; therefore, some of them are included in large and intermediate volcanoes. Novae are characterized by radial fracture zones, which mainly are grabens forming on positive landforms. Fifty novae were discovered on Venus, with diameters between 50 and 300 km. Novae usually distribute in high-elevations such as Atla and the west of Aphrodite, or occur together as clusters such as the Themis region. Novae, large volcanoes, anemones, and coronae tend to appear together, encircle, and encompass each other.

Venus has different types of lava flows (Figure 6), including effusive lava flows, lava channels, and festoon lava flows, formed by the superposition of multiple eruptions of high-viscous lava. Lava flows on Venus have a length between several to several hundred kilometers. They originated from volcanic craters, crustal fissures, or surface depressions. However, in most cases, the source of lava flows could not be recognized because of the continuous eruption and overlapping of lava flows. The surface of lava flows is smooth developing with lava channels, levees, compressional ridges, and flow fronts, indicating the flow directions. Lava channels with a length of hundreds to thousands of kilometers are abundant in lava plains. Simple lava channels have few to no branches. Canal-like lava channels usually occur in an area with low reliefs; they have large width-to-depth ratios and could keep constant for a long distance.

Except for the volcanic features formed in the past, volcanic activities may also happen at present. According to the Venus Express thermal emission data, Smrekar et al. (2010) studied three hot spots on Venus. Compared with adjacent areas, lava flows on these three hotspots have higher thermal emission intensities, indicating Venus may have young volcanism. According to the Magellan radar and microwave thermal emission data, Bondarenko et al. (2010) proposed the Bereghinia region has current volcanism, likely representing mafic eruptions. In addition, the monitoring of SiO_2 contents in the atmosphere (e.g., Esposito, 1984; Marcq et al., 2013), the oxidation experiment of olivine (e.g., Filiberto et al., 2020), and the evolution model of coronae (Gülcher et al., 2020) provide indirect evidence to the current hot spot activities on Venus.

2.4 Volcanism on Mars

Mars has 1/9 mass and 1/2 radius of the Earth, its density (3.933 g cm^{-3}) and surface gravitational acceleration (3.72 m s^{-2}) are also smaller than those of the Earth. Due to the smaller gravity and no magnetic field, the atmosphere of Mars is very thin and mainly composed of carbon dioxide (95%). The average surface atmospheric pressure of Mars is about 6.1 mbar (1 mbar=10^2 Pa). The Martian topography is dichotomous (Figure 7), with the southern part being higher and the surface relatively older, while the northern part is lower and younger (Xiao, 2013). The surface of Mars is rich in volcanic, fluvial, and glacial landforms, and is an important site for extraterrestrial habitats and life detection.

The volcanic units, covering about 22% of the Martian

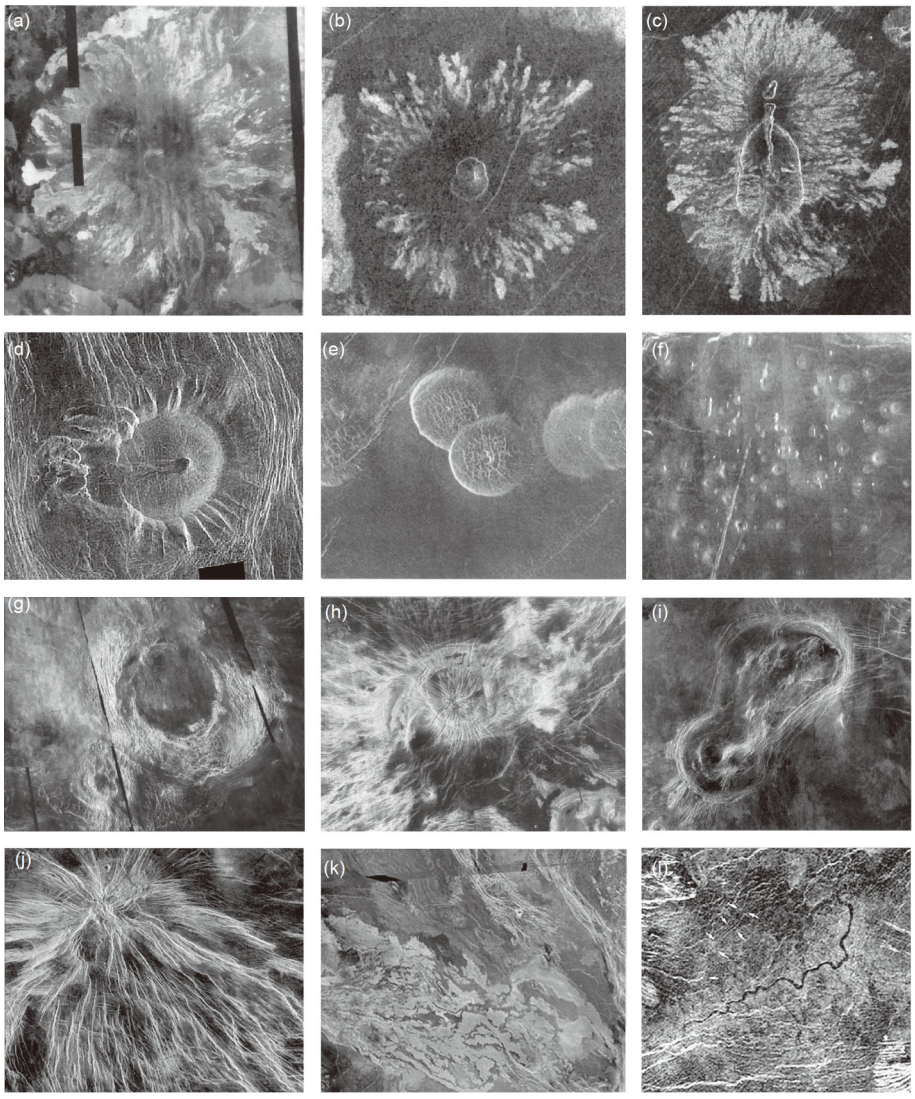

Figure 6 Typical volcanic features on Venus. (a) Large volcano with a diameter of 520 km; (b) intermediate volcano with a diameter of 38 km; (c) anemone-shaped volcano with a size of 40 km×60 km; (d) tick-shaped volcano with a diameter of 65.6 km; (e) pancake-shaped volcanic dome with an average diameter of 25 km; (f) cluster of small shield volcanoes distributed in an area of 129 km; (g) concentric corona with a diameter of 370 km; (h) radial corona with a diameter of 175 km; (i) multiple classes corona with a size of 380 km×200 km; (j) nova with a diameter of 250 km; (k) one of the longest lava flows on Venus, with a length of 1000 km; (l) lava channel distributed in an area of 30 km×190 km. All figures are north up. Basemaps are based on the NASA Magellan mission.

surface (Tanaka et al., 2014), are mainly located on the southern plateau of Mars (Figure 7), including Tharsis, Circum-Hellas central volcanic regions and widespread lava plains, and the most prominent central volcanic region in the northern plains is Elysium region (Xiao and Greeley, 2008). In addition, a large number of small conical features termed pitted cones, with diameters less than 1 km, are widely distributed in the transition region between the northern lowland and southern highland (Ivanov et al., 2014; Ye et al., 2021; Zhao et al., 2021). There are various origins for these pitted cones, such as cinder/scoria cones, tuff cones/rings, maars, rootless cones, and pingos (de Pablo and Komatsu, 2009; Hamilton et al., 2011; Ivanov et al., 2014). The pitted cones are important geological features for testing the paleo-oceanic hypothesis of the northern Martian plains.

Shield volcanoes are the most typical volcanic constructions on the surface of Mars, with broad, gentle slopes and large bases, and an overall shield-like shape. There are widely distributed shield volcanoes in the south and north hemispheres of Mars, such as Olympus and Alba Mons in the Tharsis region (Figure 8a), Elysium, Hecates, and Albor in Elysium region (Figure 8b), and Tyrrhena, Hadriaca, and Amphitrites in the Circum-Hellas region (Figure 8c). Among them, Olympus with a height of 22 km is the highest volcano in the Solar System, and Alba has a basal diameter of more than 2,000 km and a very small slope (~0.5°). All of these shield volcanoes are formed by the effusive eruptions of magma. Pateras are some depressions similar to large impact

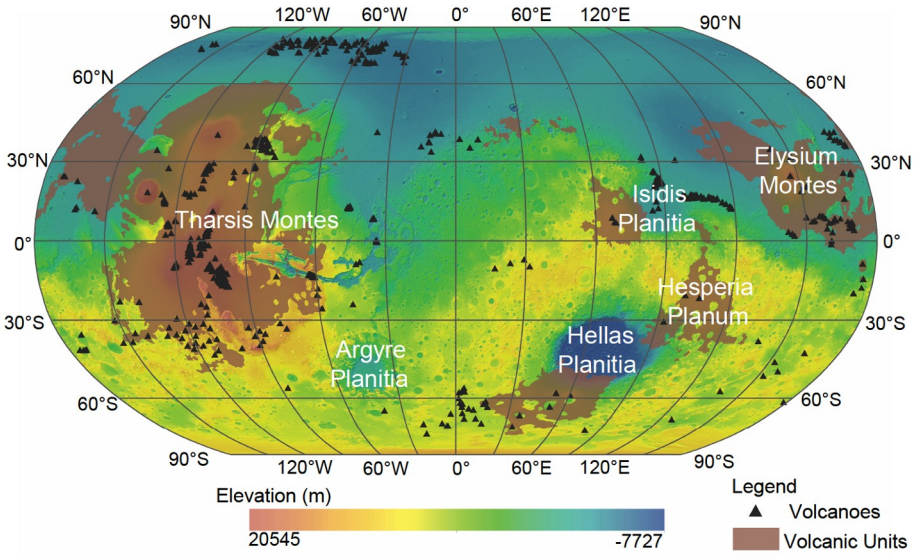

Figure 7 Map of Martian global volcanoes and volcanic units. The basemap is the MOLA DEM overlaid on the MOLA shaded relief. According to Tanaka et al. (2014) and Byrne (2020), Copyright © 2019 Springer Nature.

craters, but they absent prominent impact crater rims. Typical paterae in the Circum-Hellas region are Peneus, Malea, and Pityusa (Figure 8c, 8d). There are usually wrinkle ridges and valleys around the paterae, which indicate they may be the same as calderas on Earth. It is generally believed that these paterae are formed as a result of explosive eruptions of rising magma interacting with groundwater (Brož et al., 2021). The low atmospheric pressure of Mars favors the fragmentation of rising magma, so explosive eruptions should be common (Head and Wilson, 1998), but actual evidence of explosive volcanism on Mars is scarce (Brož et al., 2021). Apollinaris Mons (Figure 8e), located to the north of the Gusev impact crater, may be explosive volcanic in construction, with the fan-shaped deposits on its southern flank likely being volcanic debris material (Brož et al., 2021).

In addition to the large-scale volcanic edifices, a wide range of small cones can be observed in the high-resolution images. There are various cones formed by small-scale magmatic activities, such as scoria/cinder cones, small-vent fields, and fissure vents in the Tharsis region (Bleacher et al., 2007; Brož et al., 2015) (Figure 8f–8h). In the northern plain of Mars, widely distributed pitted cones with a possible origin of mud volcanoes have attracted the attention of many scholars (Ivanov et al., 2014; Salvatore and Christensen, 2014; Ye et al., 2021). The pitted cone is also a prominent feature in the Zhurong landing region (Zhao et al., 2021) (Figure 8i). It is controversial the origin of the pitted cones, the possible origins include rootless cones (Fagents et al., 2002; Frey and Jarosewich, 1982), ice core mounds (de Pablo and Komatsu, 2009; Dundas and McEwen, 2010), and volcanic debris cones/rings (Brož and Hauber, 2013), all of which are associated with groundwater/water ice and are important for the study of the habitable environment and life on Mars.

Using impact crater size-frequency distribution statistics, the ages of moderate and large volcanoes across the Martian globe have been obtained (Werner, 2009; Robbins et al., 2011; Xiao et al., 2012). These chronological studies show that vigorous eruptive volcanoes developed extensively across the globe during the Noachian, and that volcanism was concentrated in the Tharsis, Elysium, and Circum-Hellas basins as energy was dissipated throughout the planet. Subsequently, volcanism in the Circum-Hellas basin ceased during the early Hesperian, and volcanism in the Elysium region continued until about 500 Ma. Finally, only volcanism in the Tharsis region continued from 1.6 Ga to 100 Ma. In recent years, with the acquisition of new data, especially the analysis of seismic data from the Insight lander, it has been found that there are active geological formations in the Cerberus Fossae region, southeast of Elysium Mons. Interestingly, this region shows the youngest volcanic activity on the Martian surface, with a probable latest activity age of 53 to 210 ka (Horvath et al., 2021). By analyzing the topography, iron distribution, and tectonics, Broquet and Andrews-Hanna (2022) assumed that active mantle column structures still exist in this region.

Because most of the central volcanic regions are covered with thick dust (Christensen et al., 2001), it is not available to conduct direct spectral observations of the rock composition of these volcanic regions. The lower slope is strongly indicative of lower magmatic viscosity (Plescia, 2004). Based on morphological and chronological studies of these volcanoes, the composition of overflow lavas has been analyzed: global (Bandfield et al., 2000; Rogers and Christensen, 2007; Ody et al., 2012) and local (Christensen et al., 2005; Rogers and Nazarian, 2013; Huang and Xiao, 2014) mineralogical

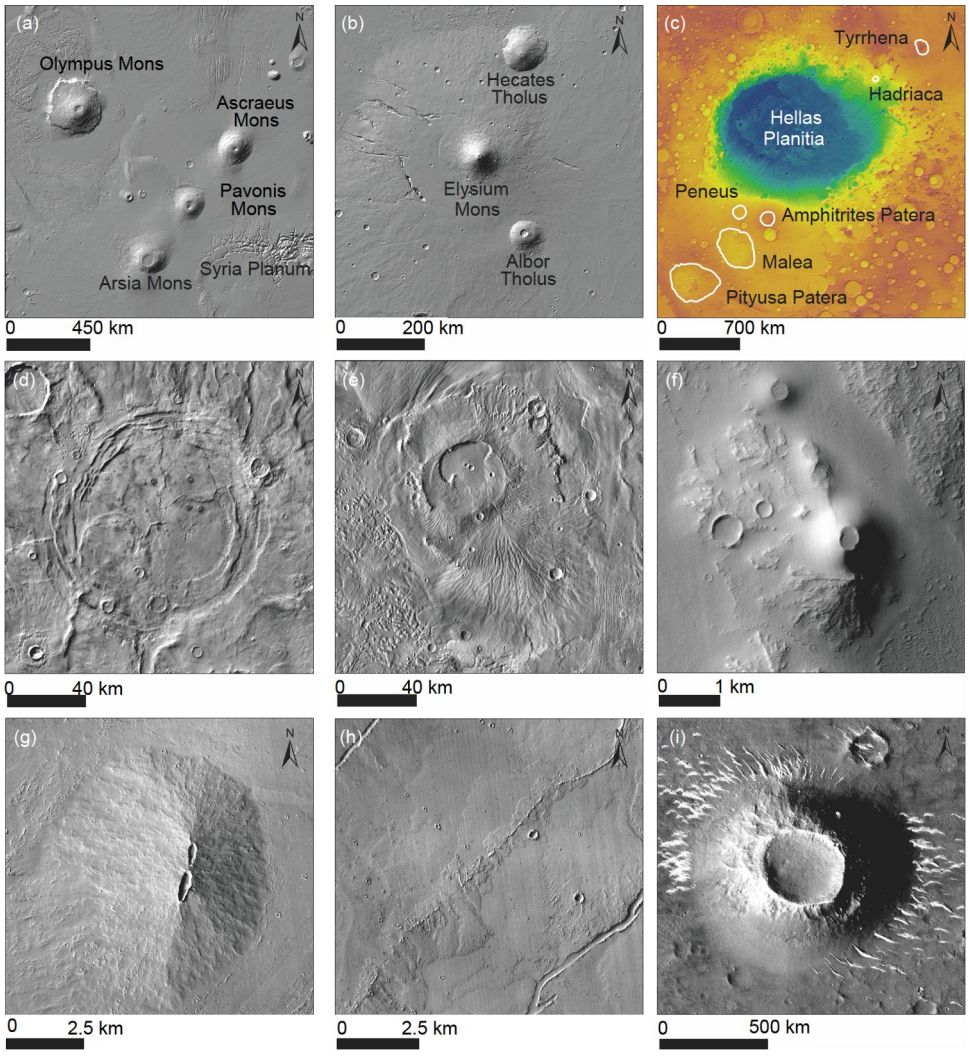

Figure 8 Typical volcanic landforms of Mars. (a) Major volcanic edifices in the Tharsis region. The basemap is the MOLA shaded relief. (b) Major volcanic edifices in Elysium region. The basemap is the MOLA shaded relief. (c) Major volcanic landforms in the Circum-Hellas volcanic region. The basemap is MOLA DEM overlaying a shaded map. (d) Peneus patera in Circum-Hellas region. The basemap is the THEMIS daytime global mosaic. (e) Apollinaris Mons, THEMIS daytime global mosaic at the bottom. (f) A putative cinder cone in the Tharsis volcanic region. The base map is CTX global mosaic. (g) Small-vent fields in the Tharsis region. The basemap is CTX global mosaic. (h) Fissure vents in Tharsis region. The basemap is CTX global mosaic. (i) A pitted cone in the Zhurong landing zone. The basemap is a digital image from the Tianwen-1 high-resolution camera (HiRIC DIM).

compositions were obtained using thermal infrared and visible/near-infrared spectral data from orbital remote sensing of Mars, and the vast majority of lava compositions were found to be basaltic, consisting of olivine, clinopyroxene, orthopyroxene, plagioclase, and high-silica-phase minerals (e.g., glass, zeolite, and phyllosilicate) in varying amounts. The global distribution of H, Si, Cl, K, Fe, and Th elements at 45° north and south latitudes was obtained using gamma-ray spectrograph (Boynton et al., 2007; El Maarry et al., 2009; Gasnault et al., 2010), and some differences in elemental composition were found among the different volcanic provinces, probably due to different degrees of the molten martian mantle. So far, more evolved magmas than basalts occur in a small lava flow in the Syrtis Major region (Christensen et al., 2005). Although orbital (Carter and Poulet, 2013; Wray et al., 2013) and *in-situ* (McLennan et al., 2014; Vaniman et al., 2014) surveys have found plagioclase-rich material, they may be remnants of exposed plagioclase crust.

It has been controversial for a long time whether the dominant composition of the upper Martian crust is lava formed by effusive volcanism (McEwen et al., 1999; Beyer and McEwen, 2005) or pyroclastics formed by explosive volcanisms (Bandfield et al., 2013). The discovery and interpretation of super-volcanoes (Michalski and Bleacher, 2013) and knobs on ancient volcanoes in the southern highlands (Huang and Xiao, 2014) support the idea that pyroclastics are the prominent component of the upper crust, suggesting that explosive eruptions likely dominated early Martian volcanism (Bandfield et al., 2013; Huang and Xiao, 2014). In addition, according to the topographic and gravity inversions, there may be a large amount of effusive lava (Grott and Wieczorek, 2012) under the loose eruptive ma-

terials of Tyrrhena which has been proposed typical explosive volcano. Therefore, the approximate proportions of denser lava and looser volcanic debris in the Martian upper crust and their respective horizontal and vertical distributions need to be further investigated.

3. Volcanism of outer Solar System bodies

The outer Solar System planets are composed mainly of hydrogen and helium and with no associated volcanic activity observed. However, their moons are usually composed of solid materials such as rocks and ice, which have been detected by the Voyager, New Horizons, Galileo, and ground-based telescopes. The vast amount of image data obtained by Voyager, New Horizons, and Galileo probes and ground-based telescopes indicate that Io's surface is volcanically active and that large amounts of magma are ejected from Io's interior by Jupiter's tidal heating, creating large craters and extensive lava flows. In addition, ice volcanic eruptions on the surfaces of icy moons and dwarf planets such as Io, Titan, Triton, Ceres, and Pluto may be the result of water and gas ejected from the subglacial ocean along the ice fissures by tidal forces, which is important for astrobiological studies.

3.1 Io

Io is one of the moons of Jupiter, similar in size to the Moon (radius 1,822 km) but with a higher density (3,528 kg m^{-3}) and a large amount of sulfurous material on its surface. Io is the most volcanic body in the Solar System, with ~30 times more heat flow than the present-day Earth, and about 55% of the heat flow originates from volcanic hot spots. A large number of active volcanic centers can be observed on the surface of Io from ground-based visible/near-infrared images and enhanced thermal emission data acquired by the probe at close range (de Pater et al., 2021). These volcanoes vary greatly in eruption type, duration, and intensity (Davies et al., 2001). More than 250 volcanic centers have been identified on the surface of Io based on multi-source data obtained by the probe (Veeder et al., 2012, 2015), including a large number of volcanism-related hot spots and paterae (Hamilton et al., 2013) (Figure 9).

The volcanic landscape and heat flow on Io are not randomly distributed. Previous studies have found a very complex spatial distribution of volcanic centers, hot spots, and mountains (Keane et al., 2018; de Pater et al., 2021), and many authors have suggested that this particular distribution pattern is related to the location and form of tidal heat release in Io's interior. The successive eruptions of a series of large volcanoes in the same region on Io (de Pater et al., 2016, 2021) suggest that these volcanic regions are linked by similar burial depths of a magma chamber or by earthquakes triggered by a particular volcanic activity. Currently, there are too little data on Io to perform statistical analyses to explain this phenomenon, but previous studies have reported that one volcanic event on Earth triggered the eruption of another volcano several hundred kilometers away (Linde and Sacks, 1998). Thus, the volcanism of Io may also have a chain effect.

Sudden, violent eruptions of magma form lava fountains, which are short-lived and preceded by low thermal anomalies that are difficult to capture on ground-based telescopes with low time sampling frequencies. The lack of atmosphere on Io makes it possible to produce violent eruptions even with low volatile content in the magma (Wilson and Head, 1981). The Galileo probe observed erupting lava fountains at Tvashtar Paterae in November 1999 and February 2000 (Figure 10a, 10b), finding magma erupting from 25 km-long fissures up to ~1 km in height (Keszthelyi et al., 2001; Milazzo et al., 2005; Davies, 2010), demonstrating that sudden exothermic events on the surface of Io are associated with violent eruptions of lava fountains. The temperature of the active lava flow on the surface of Io is about 1,200–1,500 K (Johnson et al., 1988; Veeder et al., 1994) which is similar to the basaltic magma (1,300–1,450 K) on Earth. Galileo observed that the eruption of Pillan patera (McEwen et al., 1998; Davies et al., 2001) (Figure 10c, 10d) generated lava with a temperature of about 1,825 K (McEwen et al., 1998) which was similar to the ultrabasic magma (1,700–1,900 K) on Earth. Another possible high-temperature ultramafic eruption numbered 201308C (de Kleer et al., 2014) was observed by the ground-based telescope in 2013 (Figure 10). Previous spectral analyses using 1.98 to 4.07 μm revealed a widespread distribution of sulfur dioxide frost on the Io surface (Carlson et al., 1997; McEwen et al., 1998; Laver and de Pater, 2009). Further studies have shown that the coarser grains of sulfur dioxide frost are distributed near the equator, while the finer grains are distributed at higher latitudes (Geissler et al., 2001; Laver and de Pater, 2009), and that these materials were likely formed by volcanic eruptions.

Io and Earth are the only objects in the Solar System where active silicate volcanic eruptions have been observed (Tyler et al., 2015), with Earth's volcanism relying on the energy released from radioactive elements, while Io's surface eruptions rely primarily on frictional heating from tidal interactions with Jupiter. Traditional models of tidal heating assume that the interior of Io is mainly solid, with almost all of the heat generated diffusing into the solid layer. However, newer studies suggest that the heat generated by tidal action diffuses mainly into the liquid layer, meaning that the interior of Io is not completely solid and may contain layers similar to magma oceans (de Pater et al., 2021). The presence of a subsurface liquid layer of Io allows for multiple diffusion patterns of tidal heating and may be more conducive to the

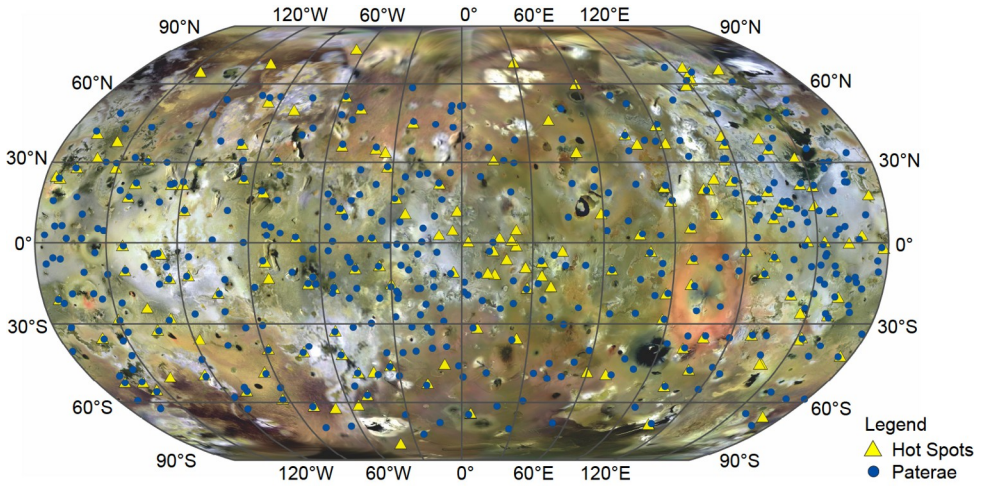

Figure 9 Distribution of hot spots and caldera-like paterae on Io. According to Hamilton et al. (2013). The basemap is the Io global merged mosaic of images from Galileo and Voyager.

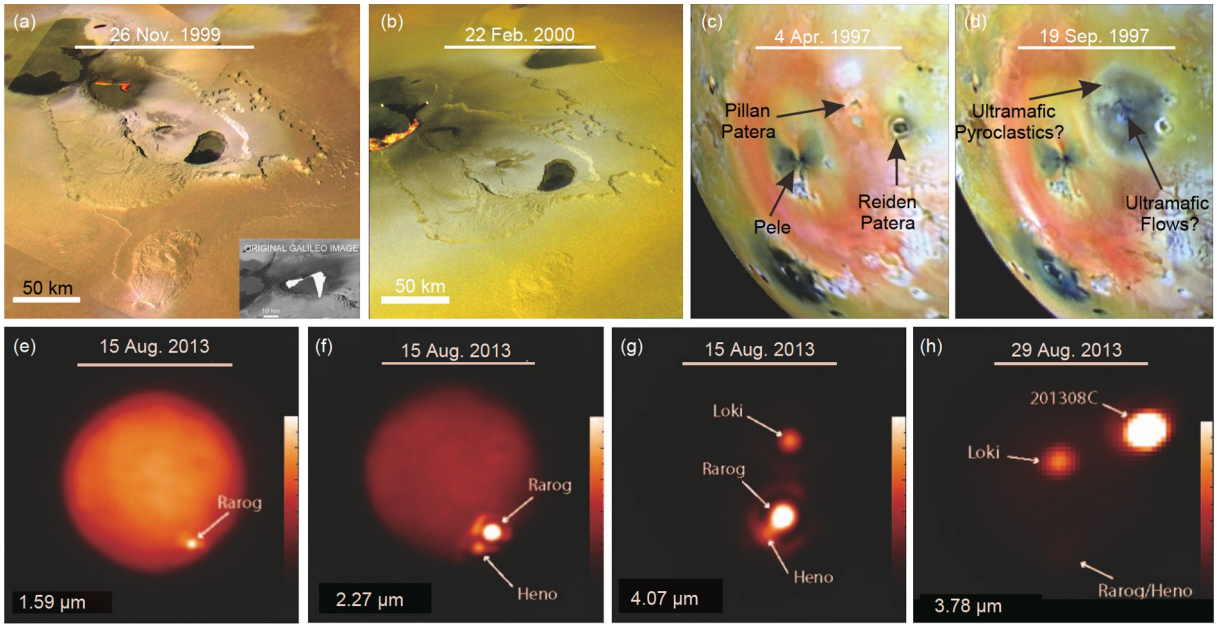

Figure 10 Typical volcanic activities on Io. (a), (b) Two lava fountain eruptions in 1999 and 2000 at Tvashtar Paterae. The lava flow in (a) is an illustration based on real data in the lower right corner. Sources are NASA PIA02545 and PIA02550, respectively. (c), (d) Comparison of before and after the eruption of the Pillan Patera. Modified from NASA PIA00744. (e)–(h) Ground-based remote sensing images of Io at different thermal infrared wavelengths. (e)–(g) were taken by the 10-m Keck II telescope of W. M. Keck Observatory on August 15, 2013. (h) was taken by the Northern Gemini Telescope on August 29, 2013. These images show the thermal infrared emission characteristics of Io's surface at the time of the eruption of Rarog, Heno, Loki Paterae, and 201308C. The color bar on the right side of the figure indicates the intensity of the thermal emission. Adapted from NASA PIA18656.

development of surface hotspot volcanoes than the traditional solid layer.

At present, the following scientific questions remain in the study of Io. What are the extent, material composition, and morphology of Io's core, mantle, and lithosphere? Whether there exist magmatic oceans in Io's subsurface? What are the size and spatial distribution of Io's heat flow, and can it be reflected by surface heat flow and geological features? Where does Io's tidal heat originate in its interior, the asthenosphere, the deep mantle, or the magma ocean? What is the composition and chemistry of Io's magma, whether ultramafic, mafic, or sulfide, and is there a correlation with spatial location? Is Io in thermal equilibrium? How are sodium chloride and potassium chloride formed on Io, and why are they not distributed in the same region as sulfur dioxide? How do Io's volcanic eruption plumes interact with the atmosphere? What is the role of cryptic volcanism in the formation of Io's atmosphere (de Pater et al., 2021)?

3.2 Icy satellites

Many icy satellites exist around the giant planets in the outer Solar System. Such as molten magma upwells from the hot interior and erupts on the silicate crust of rocky planets, forming a volcano, vapor- or liquid-phase water (or other volatiles, often contains solid materials) upwells and erupts on the icy crust of icy planets/satellites, forming a cryovolcano or an ice volcano. This cryovolcanism resulted from the upwelling of molten icy materials continuously resurfacing the icy planets/satellites and can reveal the internal structures and thermal evolution histories of these astronomical bodies (Kargel, 1991; Schenk et al., 2001; Quick et al., 2017). Cryovolcanism has been found on many dwarf planets and icy satellites in the Solar System, such as Ceres, Europa, Ganymede, Enceladus, Titan, Miranda, Triton, and Charon (Geissler, 2015). The Voyager 2 reveals the first icy satellite with an active cryovolcano—Triton. A geyser-like volcanic plume is presented on this icy satellite, spewing nitrogen gas. The Cassini-Huygens mission found spectacular saltwater plumes erupting from Enceladus and lakes of methane and other volatiles that probably erupted from the icy interior of Titan. Hubble Space Telescope observations have detected a water vapor plume from Jupiter's moon Europa. Evidence of past cryovolcanism was also found on other icy astronomical bodies. Cryovolcanism is widespread and extremely varied. Some cryovolcanic landscapes are similar to many silicate volcanic terrains, including what appear to be volcanic rifts, calderas and solidified lava lakes, flow fields, breached cinder cones or stratovolcanoes, viscous lava domes; while many others exhibit no obvious volcanoes (Kargel, 1995). Cryovolcanism is generally believed to have formed by eruptions of aqueous solutions and slurries. Even on the surface mainly consisting of solid nitrogen, that is, Triton's, "cryomagma" is probably dominated by water ice. Nonpolar and weakly polar molecular liquids (mainly N_2, CH_4, CO, and CO_2) may have erupted on some icy satellites, but without water, these substances do not form rigid solids that are stable against sublimation or melting over geologic time (Kargel, 1995). The Uranian and Neptunian satellites have cryovolcanic deposits that are hundreds to thousands of meters thick; by contrast, the Jovian and Saturnian satellites generally have plains-forming deposits composed of relatively thin flows. This distinction suggests that the cryomagma on Jovian and Saturnian satellites tend to have a relatively higher fraction of water ice and thus lower viscosities, while the cryomagma on Uranian and Neptunian satellites may possess large amounts of a chemically unequilibrated volatile assemblage and maybe silicate particles. Furthermore, gas clathrate hydrates may play important roles in many aspects of cryovolcanism, but strongly affect the viscosity. Studies have found that gas clathrate hydrates could be present in the crusts of Titan (Lunine and Stevenson, 1985), Pluto (Kamata et al., 2019), and Ceres (Fu et al., 2017).

It has been widely accepted that two conditions must be met for cryovolcanic activity to take place: melts can be generated in the interior, and the melts can migrate to the surface of the planet/satellite. Lowering the eutectic point by adding salt is a crucial mechanism of melting ice at very low temperatures. This mechanism could play a significant role in the cryovolcanism on Ceres and Pluto, where solar heating the probably the only energy source (Castillo-Rogez et al., 2018). Many heating mechanisms contribute to the melting in the interiors. The most important energy sources are gravitational, radiogenic, and tidal. Besides, solar heating probably drives the nitrogen plumes on Triton. Therefore, the planetary factors that determine whether cryovolcanism can occur include size, composition (determines radiogenic heating), location in the Solar System (related both to composition and surface temperature), and the history of the orbit of the planet/satellite (related to tidal hearing). Several missions since the 21st century have obtained plenty of observations of icy planets/satellites, some of which are introduced in the following subsections.

3.2.1 Europa

Europa, with a radius of 1565 km, is primarily composed of silicate rocks plus a small fraction of lighter materials. Prior to the Voyager mission, radar observations from the Earth suggested the presence of ice on Europa. In 1979, Voyager 1 and 2 arrived at Jupiter and obtained detailed images of the Galilean satellites. Based on the data from the Voyager mission, the surface of Europa was mainly classified as chaos terrains or plains. Europa shows a bright icy surface with long and dark streaks, several tens of kilometers wide, crisscrossing the entire globe. The surface features have been attributed to extensive cryovolcanism (Lucchitta and Soderblom, 1982; Squyres et al., 1983).

In 1996, the arrival of the Galileo space probe at Europa brought back more data and gave rise to a heat wave of Europa studies. Based on the Galileo data, the existence of a subsurface ocean beneath the icy crust of Europa was confirmed (Khurana et al., 1998; Kivelson et al., 2000). With the subsurface ocean, many researchers tended to ascribe the surface features to cryovolcanism, including (1) apparently lobate "flows" (Figure 11a), (2) certain elliptical to circular lenticulae (Figure 11b), and (3) low-lying, smooth, low-albedo surfaces (Figure 11c), which are probably originated from cryovolcanism (Fagents, 2003). After the Galileo mission, using the Hubble Space Telescope, some studies aimed to find evidence of cryovolcanism activities. Roth et al. (2014) found line emission from the dissociation products of water. Sparks et al. (2016, 2017) found evidence for off-limb continuum absorption as Europa transited Jupiter. These findings suggest Europa has active plumes of water,

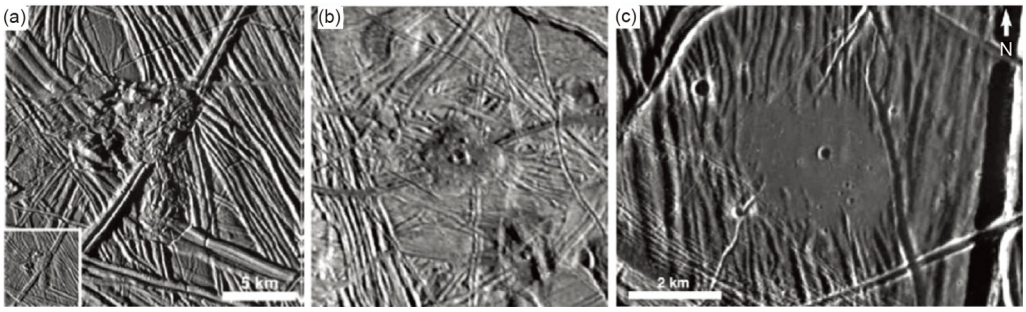

Figure 11 (a) Apparently lobate features (35°N, 88°W). (b) A lenticulae apparently superposed on the surrounding terrain (12°N, 272°W). Image resolution is ~200 m/pixel. (c) Smooth, low-albedo material occupying a topographic low (6°N, 327°W). Images are from Fagents (2003), Copyright © 2003 John Wiley and Sons.

very possibly active cryovolcanoes. The existence of cryovolcanoes provides a simple pathway connecting the shell and the subsurface ocean and is vital for Europa's habitability.

3.2.2 Enceladus

Enceladus is the sixth largest moon of Saturn and the brightest satellite in the Solar System. It is covered by ice, with an average diameter of 505 km. High-resolution images from Voyager 2 revealed at least five different types of terrain, including cratered terrain, smooth terrain, ridged terrain bordering the smooth areas, extensive linear cracks, and scarps. Given the lack of craters on the smooth plains, these regions are probably less than a few hundred million years old. Thus, in the recent geological past, Enceladus must have been active with cryovolcanism (Kargel and Pozio, 1996). Cryovolcanism was first confirmed by the Cassini-Huygens spacecraft. Huge plumes were shot from the south pole of the globe into space, taking materials about 200 kg per second at a velocity of 1.2 km s^{-1} to as far as 500 km. The plumes vent from the fractures bounded by ridges, called "tiger stripes" (Figure 12). The ice ridges are much warmer (a maximum of 180 K) than the surroundings. The brightness of the plumes varies significantly with the position of Enceladus in its orbit. The plumes are the brightest when Enceladus is at apoapsis, suggesting the mechanism that drives the eruptions is due to tidal forces. Cassini flew through the plumes three times and directly analyzed their composition: vapor-phase mass includes 90% H_2O, 5% CO_2, 1% CH_4, and 1% NH_3, as well as trace amounts of hydrogen and organic molecules; solid-phase mass contains mainly ice frozen from brine, with 1% NaCl (Hansen et al., 2011; Waite et al., 2017). Since salt precipitates, while water freezes to ice, containing salt in the plumes indicated that the plumes were not from the icy shell of the globe, but directly vented from the liquid water beneath. Considering the organic molecules, many researchers suspected that the subsurface ocean of Enceladus may be habitable. This is a big step for exploring extraterrestrial life in the Solar System. The ocean world of Enceladus could potentially be an oasis for extraterrestrial life.

3.3 Dwarf planets

There are five widely accepted dwarf planets in the Solar System, one in the asteroid belt and four in the Kuiper belt. Only Ceres in the asteroid belt and Pluto in the Kuiper belt were explored with space missions and have abundant data, revealing some key features of cryovolcanism on dwarf planets.

3.3.1 Ceres

Ceres is the only dwarf planet and the largest body in the asteroid belt. It has a diameter of 950 km and is 2.8 AU from the sun. Although the outermost of Ceres consists of silicate rocks, the shallow subsurface should be a mixture of 30–40% ice and 60–70% rocks (Bland et al., 2016). While deeper in Ceres, between the subsurface and the rock inner core, a "mantle" layer made of purer ice may exist (Castillo-Rogez and McCord, 2010). Many researchers believe that the mantle of Ceres mainly consists of silicate hydrates, while liquid water may exist in the porous rocks of the "upper mantle" (Castillo-Rogez et al., 2020), and brine may exist in liquid-storage regions at the crust-mantle boundary (Raymond et al., 2020). In 2015, the Dawn spacecraft orbited Ceres, making it the first icy planet that was investigated in-orbit. The Dawn spacecraft found a dome-shaped mountain with a height of ~4 km on the surface of Ceres. This predominant mountain, named Ahuna Mons, was taken as a cryovolcano (Figure 13).

The life cycle of Ahuna Mons was investigated by various studies (e.g., Ruesch et al., 2016). Many proposed that cryovolcanic domes, less viscous than the icy crust, viscously relax due to gravity over geologic timescales, precluding constructs older than Ahuna Mons from easy identification (Sori et al., 2017). Based on this assumption, Sori et al. (2018) identified many domes that were old cryovolcanic constructs, estimated their ages, and proposed an average cryomagma extrusion rate of ~10^4 m^3 yr^{-1}. Ruesch et al. (2019) analyzed a gravity anomaly associated with the geologically recent dome Ahuna Mons, and determined that the subsurface structure includes a regional

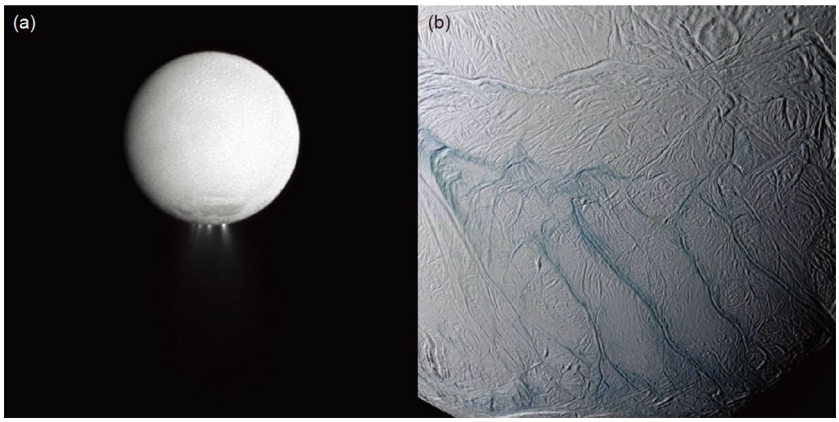

Figure 12 Enceladus. (a) The plumes vented from the south pole. (b) Tiger stripes. Images from NASA/JPL-Caltech/SSI.

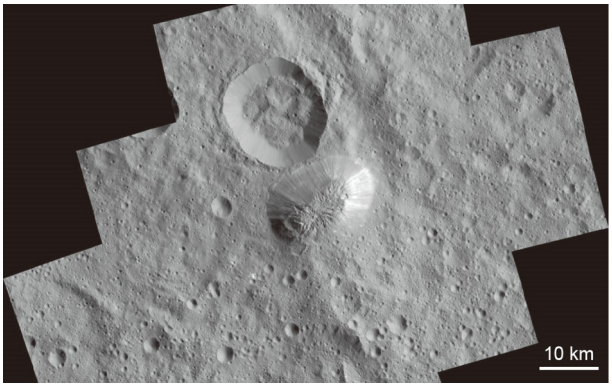

Figure 13 Ahuna Mons imaged by the Dawn spacecraft. The diameter of the mountain is about 20 km, and the average height is 4 km. North is up. Image from NASA/JPL-Caltech.

mantle uplift, which was interpreted as a plume by the authors. Such a plume could be a slurry of brine and rock particles. Studies believe that such slurry-like material extensively exists and convects in the mantle of Ceres (Travis et al., 2018), and thus, causing cryovolcanism. Moreover, studies also consider gas hydrates as a low-density, high-strength component in the crust of Ceres. Gas hydrates could significantly slow down the cooling, help sustain a liquid-phase and affect the internal structure of Ceres (Castillo-Rogez et al., 2019; Hesse and Castillo-Rogez, 2019). While the release of gas will strongly enhance cryovolcanism (Quick et al., 2019), the presence and uniqueness of Ahuna Mons reveal the volcanism on Ceres. The evolution history of Ceres is an important reference for the understanding of icy satellites in the Solar System and also aids the understanding of the evolution of terrestrial planets from a different perspective.

3.3.2 Pluto

Pluto, a dwarf planet in the Kuiper belt, is the largest and second most massive dwarf planet known in the Solar System. It is about one-sixth of the moon in mass and one-third of the moon in volume. With a radius of about 1188 km, Pluto has a rock core, and the outermost 300 km mainly consists of rock and ice (Grundy et al., 2016; McKinnon et al., 2017). During the fly-by of the New Horizon spacecraft in July 2015, plenty of images and composition data were obtained. This dwarf planet was found not to be a totally frozen world, but has many mountains and plateaus (for example, Voyager Terra), and a vast and flat plain (Sputnik Planitia), suggesting tectonic, glacial, and even cryovolcanic activities (Moore et al., 2016). At a temperature of 35–60 K and a pressure of ~10 μbar on the surface of Pluto, water, methane, carbon monoxide, ammonia, and nitrogen are way below their triple points, respectively, and thus, freeze into ice. At such temperature and pressure, pure-water ice is very rigid, forming bedrock that is unable to flow. When other volatiles (such as ammonia) or salt are added to water ice, water ice becomes flowable in short geological time scales, such as on Earth (Cruikshank et al., 2019). Recently, Singer et al. (2022) found many dome structures, at least 7 km in height and 100 km in width, that are unique to Pluto. These authors believe that these structures indicate geological activities related to cryovolcanism. Such as Wright Mons, spectrometry studies suggest it is rich in volatiles, including water ice, methane, and nitrogen (Figure 14a–14e). Previously, Pluto was believed to have lost its internal heat long age, but the evidence of cryovolcanoes indicates that it could maintain enough heat to induce geological activities that are quite late. This finding implies that cryovolcanism could exist on more icy astronomical bodies, and the hear sources and evolutions on the icy astronomical bodies need re-investigations.

In the research of cryovolcanism on icy planets/satellites, observations are all from the surface. Since landing and sampling missions are still extremely difficult, many models and simulations on the flow of ice bodies depend on the rheology of ice. Understanding the rheological behavior

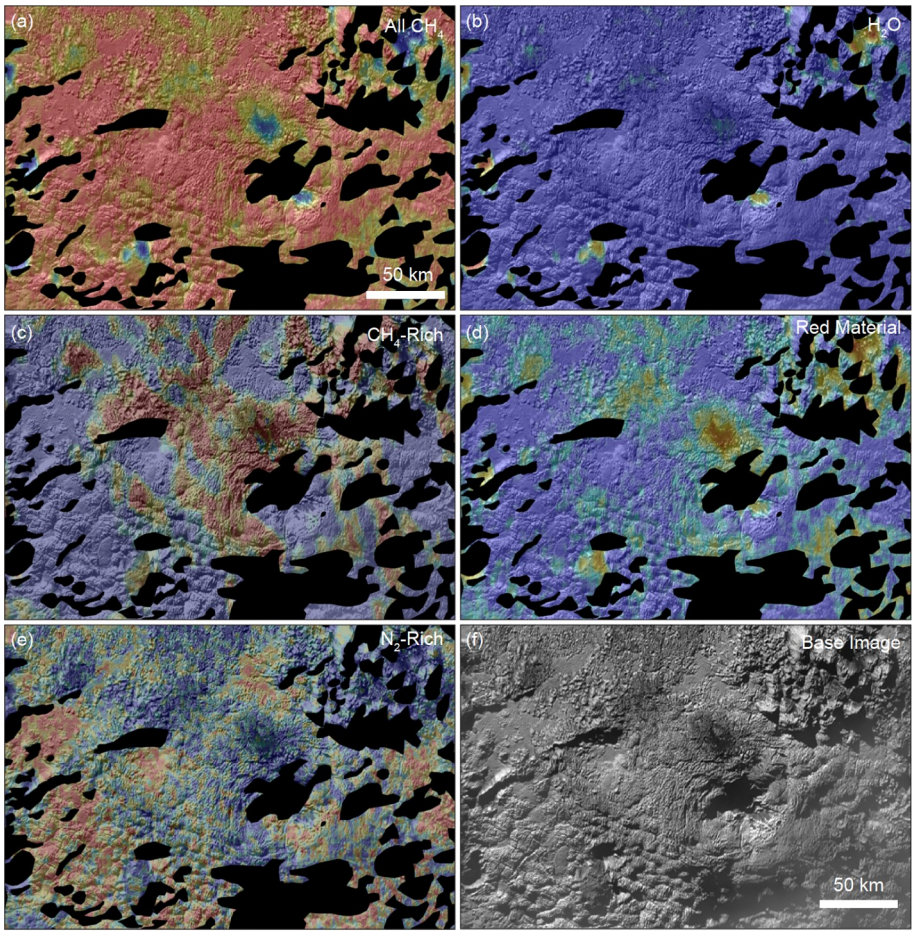

Figure 14 Composition maps of Pluto using the LEISA spectrometry data on New Horizon. This region is Wright Mons. In all panels, redder color means stronger absorption, indicating more content of the material. (a) Methane. (b) Water ice. (c) Regions where methane is higher than nitrogen. (d) Organic matters. (e) Regions where nitrogen is higher than methane. (f) Topographic map in gray scale. Figure from Singer et al. (2022), Copyright © 2022 the Author (s).

of ice enables further exploration of the composition, structure, and evolution history of these icy planets/satellites. Although ice has many solid phases, ice Ih (phase I hexagonal) is the only stable phase below 200 MPa and between 72 and 273 K. In the Solar System, except for the possible existence of high-pressure phase ice II in deep Ganymede and low-temperature phase ice XI in cold regions of Pluto, ice on all other astronomical bodies is phase Ih. The flow of pure ice has been well studied with some marked results (Glen, 1952, 1955; Goldsby and Kohlstedt, 2001), but planetary ices are mostly impure. Ice can be mixed with dust and sands, i.e., rock particles, and also methane and nitrogen ice. Moreover, methane and ammonia can associate with ice (water) and form gas hydrates, the structure and deformation of which also play an important role in cryovolcanism. Therefore, in order to explore the movement, relaxation, and internal structure of these ice bodies, understanding the influences of impurities on the flow of ice is essential (Durham et al., 1992; Qi et al., 2018). This is a major future focus of ice physics in planetary sciences.

4. Conclusion

The Moon is the only extraterrestrial planet with returned samples; Apollo, Luna, and Chang'e-5 missions returned a total of 384 kg lunar samples. On the basis of the returned samples, scientists proposed the lunar magma ocean model and revealed the lunar mantle properties and volcanic eruption processes. However, the current samples cannot solve all key questions in lunar volcanology, including the end of lunar volcanism. Are irregular mare patches and ring moat dome structures products of Imbrian-aged or recent volcanic activities? Where are the youngest mare basalts on the Moon? Only samples from those regions were returned that could solve such significant questions in lunar volcanism.

The role of volcanism on the climate of Mars and its habitability in the geological history is the key scientific question in future research of Mars volcanism and exploration, including the contribution of a volcanic eruption to the inventory of water, the influence of CO_2, methane and other erupted greenhouse gases to the Mars climate, the transition from early-stage explosive to late-stage effusive volcanism.

The knowledge of volcanic rocks on Mercury is very limited; the resolution and detection depth of the MESSENENER element data are not precise enough to distinguish the difference between localized volcanic rocks. In addition, there are lots of unknowns for the early thermal evolution of Mercury, including the volcanic eruption phases, styles, and fluxes. Therefore, high-resolution composition data, *in situ* data, and returned samples are needed to improve the understanding of the composition, physical property, melt generation mechanism, and evolution path of volcanic rocks on Mercury.

Due to the severe surface environment (high pressure, high temperature), Venus is the hardest planet to land in the Solar System. Only several missions of Soviet Union landed on Venus, collecting a little amount of data. Except for that, the Megallen mission of NASA once orbited Venus and obtained lots of data; but because of the dense atmosphere of Venus, they are mostly based on radar, whose results usually have multiple explanations. After the Megallen mission, the exploration of Venus is not active, but more missions are on the way from NASA and ESA, such as VERITAS, DAVINCI+, and EnVision missions. The exploration of Venus will have a prosperous period at the end of 2020s, with the potential to solve more significant questions in the volcanism of Venus.

Ice, the solid phase of the most common compound in the universe, constitutes a major part of many astronomical bodies beyond the snow line. Cryovolcanism, continuously resurfacing these icy astronomical bodies, is a good subject and an important approach to studying the structure and evolution of these bodies. Meanwhile, by comparison, this research could improve the understanding of the volcanism on the Earth, which is a key area of planetary geology, planetary physics, and astrobiology.

Acknowledgements *We thank the constructive suggestions from Prof. Hejiu HUI and the three anonymous reviewers. This study was supported by the National Natural Science Foundation of China (Grant Nos. 42241111, 41773061, 41773063).*

References

Bandfield J L, Edwards C S, Montgomery D R, Brand B D. 2013. The dual nature of the martian crust: Young lavas and old clastic materials. Icarus, 222: 188–199

Bandfield J L, Hamilton V E, Christensen P R. 2000. A global view of Martian surface compositions from MGS-TES. Science, 287: 1626–1630

Baratoux D, Toplis M J, Monnereau M, Gasnault O. 2011. Thermal history of Mars inferred from orbital geochemistry of volcanic provinces. Nature, 472: 338–341

Barboni M, Boehnke P, Keller B, Kohl I E, Schoene B, Young E D, McKeegan K D. 2017. Early formation of the Moon 4.51 billion years ago. Sci Adv, 3: e1602365

Besse S, Doressoundiram A, Barraud O, Griton L, Cornet T, Muñoz C, Varatharajan I, Helbert J. 2020. Spectral properties and physical extent of pyroclastic deposits on Mercury: Variability within selected deposits and implications for explosive volcanism. J Geophys Res-Planets, 125: E2018JE005879

Besse S, Doressoundiram A, Benkhoff J. 2015. Spectroscopic properties of explosive volcanism within the Caloris basin with MESSENGER observations. J Geophys Res-Planets, 120: 2102–2117

Beyer R A, McEwen A S. 2005. Layering stratigraphy of eastern Coprates and northern Capri Chasmata, Mars. Icarus, 179: 1–23

Bland M T, Raymond C A, Schenk P M, Fu R R, Kneissl T, Pasckert J H, Hiesinger H, Preusker F, Park R S, Marchi S, King S D, Castillo-Rogez J C, Russell C T. 2016. Composition and structure of the shallow subsurface of Ceres revealed by crater morphology. Nat Geosci, 9: 538–542

Bleacher J E, Greeley R, Williams D A, Cave S R, Neukum G. 2007. Trends in effusive style at the Tharsis Montes, Mars, and implications for the development of the Tharsis province. J Geophys Res-Planets, 112: E09005

Bondarenko N V, Head J W, Ivanov M A. 2010. Present-day volcanism on Venus: Evidence from microwave radiometry. Geophys Res Lett, 37: L23202

Boynton W V, Taylor G J, Evans L G, Reedy R C, Starr R, Janes D M, Kerry K E, Drake D M, Kim K J, Williams R M S, Crombie M K, Dohm J M, Baker V, Metzger A E, Karunatillake S, Keller J M, Newsom H E, Arnold J R, Brückner J, Englert P A J, Gasnault O, Sprague A L, Mitrofanov I, Squyres S W, Trombka J I, d'Uston L, Wänke H, Hamara D K. 2007. Concentration of H, Si, Cl, K, Fe, and Th in the low- and mid-latitude regions of Mars. J Geophys Res, 112: E12

Braden S E, Stopar J D, Robinson M S, Lawrence S J, van der Bogert C H, Hiesinger H. 2014. Evidence for basaltic volcanism on the Moon within the past 100 million years. Nat Geosci, 7: 787–791

Broquet A, Andrews-Hanna J C. 2022. Is there an active mantle plume beneath Elysium Planitia? Houston: 53rd Lunar and Planetary Science Conference. Abstract#2351

Brož P, Bernhardt H, Conway S J, Parekh R. 2021. An overview of explosive volcanism on Mars. J Volcanol Geotherm Res, 409: 107125

Brož P, Čadek O, Hauber E, Rossi A P. 2015. Scoria cones on Mars: Detailed investigation of morphometry based on high-resolution digital elevation models. J Geophys Res-Planets, 120: 1512–1527

Brož P, Hauber E. 2013. Hydrovolcanic tuff rings and cones as indicators for phreatomagmatic explosive eruptions on Mars. J Geophys Res-Planets, 118: 1656–1675

Byrne P K, Ostrach L R, Fassett C I, Chapman C R, Denevi B W, Evans A J, Klimczak C, Banks M E, Head J W, Solomon S C. 2016. Widespread effusive volcanism on Mercury likely ended by about 3.5 Ga. Geophys Res Lett, 43: 7408–7416

Byrne P K, Whitten J L, Klimczak C, McCubbin F M, Ostrach L R. 2018. The Volcanic Character of Mercury. In: Solomon S C, Nittler L R, Anderson B J, eds. Mercury: The View After MESSENGER. Cambridge: Cambridge Planetary Science. 287–323

Byrne P K. 2020. A comparison of inner Solar System volcanism. Nat Astron, 4: 321–327

Carlson R W, Smythe W D, Lopes-Gautier R M C, Davies A G, Kamp L W, Mosher J A, Soderblom L A, Leader F E, Mehlman R, Clark R N, Fanale F P. 1997. The distribution of sulfur dioxide and other infrared absorbers on the surface of Io. Geophys Res Lett, 24: 2479–2482

Carter J, Poulet F. 2013. Ancient plutonic processes on Mars inferred from the detection of possible anorthositic terrains. Nat Geosci, 6: 1008–1012

Castillo-Rogez J C, Hesse M A, Formisano M, Sizemore H, Bland M, Ermakov A I, Fu R R. 2019. Conditions for the long-term preservation of a deep brine reservoir in Ceres. Geophys Res Lett, 46: 1963–1972

Castillo-Rogez J C, McCord T B. 2010. Ceres' evolution and present state constrained by shape data. Icarus, 205: 443–459

Castillo-Rogez J C, Neveu M, Scully J E C, House C H, Quick L C, Bouquet A, Miller K, Bland M, De Sanctis M C, Ermakov A, Hendrix A R, Prettyman T H, Raymond C A, Russell C T, Sherwood B E, Young E. 2020. Ceres: Astrobiological target and possible ocean world. Astrobiology, 20: 269–291

Castillo-Rogez J, Neveu M, McSween H Y, Fu R R, Toplis M J, Prettyman T. 2018. Insights into Ceres's evolution from surface composition. Meteorit Planet Sci, 53: 1820–1843

Charlier B, Grove T L, Zuber M T. 2013. Phase equilibria of ultramafic

compositions on Mercury and the origin of the compositional dichotomy. Earth Planet Sci Lett, 363: 50–60
Che X, Nemchin A, Liu D, Long T, Wang C, Norman M D, Joy K H, Tartese R, Head J, Jolliff B, Snape J F, Neal C R, Whitehouse M J, Crow C, Benedix G, Jourdan F, Yang Z, Yang C, Liu J, Xie S, Bao Z, Fan R, Li D, Li Z, Webb S G. 2021. Age and composition of young basalts on the Moon, measured from samples returned by Chang'e-5. Science, 374: 887–890
Christensen P R, Bandfield J L, Hamilton V E, Ruff S W, Kieffer H H, Titus T N, Malin M C, Morris R V, Lane M D, Clark R L, Jakosky B M, Mellon M T, Pearl J C, Conrath B J, Smith M D, Clancy R T, Kuzmin R O, Roush T, Mehall G L, Gorelick N, Bender K, Murray K, Dason S, Greene E, Silverman S, Greenfield M. 2001. Mars Global Surveyor Thermal Emission Spectrometer experiment: Investigation description and surface science results. J Geophys Res-Planets, 106: 23823–23871
Christensen P R, McSween Jr H Y, Bandfield J L, Ruff S W, Rogers A D, Hamilton V E, Gorelick N, Wyatt M B, Jakosky B M, Kieffer H H, Malin M C, Moersch J E. 2005. Evidence for magmatic evolution and diversity on Mars from infrared observations. Nature, 436: 504–509
Cruikshank D P, Umurhan O M, Beyer R A, Schmitt B, Keane J T, Runyon K D, Atri D, White O L, Matsuyama I, Moore J M, McKinnon W B, Sandford S A, Singer K N, Grundy W M, Dalle Ore C M, Cook J C, Bertrand T, Stern S A, Olkin C B, Weaver H A, Young L A, Spencer J R, Lisse C M, Binzel R P, Earle A M, Robbins S J, Gladstone G R, Cartwright R J, Ennico K. 2019. Recent cryovolcanism in virgil fossae on Pluto. Icarus, 330: 155–168
Davies A G, Keszthelyi L P, Williams D A, Phillips C B, McEwen A S, Lopes R M C, Smythe W D, Kamp L W, Soderblom L A, Carlson R W. 2001. Thermal signature, eruption style, and eruption evolution at Pele and Pillan on Io. J Geophys Res-Planets, 106: 33079–33103
Davies A. 2010. Terrestrial Lava Lake physical parameter estimation using a silicate cooling model-implications for a return to the Volcanic Moon, Io. In: EGU General Assembly Conference. 12: 5659
de Kleer K, de Pater I, Davies A G, Ádámkovics M. 2014. Near-infrared monitoring of Io and detection of a violent outburst on 29 August 2013. Icarus, 242: 352–364
de Pablo M, Komatsu G. 2009. Possible pingo fields in the Utopia basin, Mars: Geological and climatical implications. Icarus, 199: 49–74
de Pater I, Davies A G, Marchis F. 2016. Keck observations of eruptions on Io in 2003–2005. Icarus, 274: 284–296
de Pater I, Keane J T, de Kleer K, Davies A G. 2021. A 2020 observational perspective of Io. Annu Rev Earth Planet Sci, 49: 643–678
Denevi B W, Ernst C M, Meyer H M, Robinson M S, Murchie S L, Whitten J L, Head J W, Watters T R, Solomon S C, Ostrach L R, Chapman C R, Byrne P K, Klimczak C, Peplowski P N. 2013. The distribution and origin of smooth plains on Mercury. J Geophys Res-Planets, 118: 891–907
Deng Q, Li F, Yan J, Xiao Z, Ye M, Xiao C, Barriot J P. 2020. The thermal evolution of mercury over the past ~4.2 Ga as revealed by relaxation states of mantle plugs beneath impact basins. Geophys Res Lett, 47: e89051
Draper D S, Lawrence S J, Klima R S, Denevi B W, van der Bogert C H, Elardo S M, Hiesinger H H. 2021. The Inner Solar System Chronology (ISOCHRON) lunar sample return mission concept: Revealing two billion years of history. Planet Sci J, 2: 79
Dundas C M, McEwen A S. 2010. An assessment of evidence for pingos on Mars using HiRISE. Icarus, 205: 244–258
Durham W B, Kirby S H, Stern L A. 1992. Effects of dispersed particulates on the rheology of water ice at planetary conditions. J Geophys Res-Planets, 97: 20883–20897
El Maarry M R, Gasnault O, Toplis M J, Baratoux D, Dohm J M, Newsom H E, Boynton W V, Karunatillake S. 2009. Gamma-ray constraints on the chemical composition of the martian surface in the Tharsis region: A signature of partial melting of the mantle? J Volcanol Geotherm Res, 185: 116–122
Esposito L W. 1984. Sulfur dioxide: Episodic injection shows evidence for active Venus volcanism. Science, 223: 1072–1074
Fagents S A. 2003. Considerations for effusive cryovolcanism on Europa: The post-Galileo perspective. J Geophys Res-Planets, 108: 5139
Fagents S A, Lanagan P, Greeley R. 2002. Rootless cones on Mars: A consequence of lava-ground ice interaction. Geol Soc Lond Spec Publ, 202: 295–317
Fassett C I, Kadish S J, Head J W, Solomon S C, Strom R G. 2011. The global population of large craters on Mercury and comparison with the Moon. Geophys Res Lett, 38: L10202
Filiberto J, Trang D, Treiman A H, Gilmore M S. 2020. Present-day volcanism on Venus as evidenced from weathering rates of olivine. Sci Adv, 6: Eaax7445
Fitz-Gerald B. 2021. The origin of Rim Moat Domes. Lunar Section Circular, 14–28
Francis P, Oppenheimer C. 2004. Volcanoes. Oxford: Oxford University Press. 521
Frey H, Jarosewich M. 1982. Subkilometer Martian volcanoes: Properties and possible terrestrial analogs. J Geophys Res-Solid Earth, 87: 9867–9879
Fu R R, Ermakov A I, Marchi S, Castillo-Rogez J C, Raymond C A, Hager B H, Zuber M T, King S D, Bland M T, Cristina De Sanctis M, Preusker F, Park R S, Russell C T. 2017. The interior structure of Ceres as revealed by surface topography. Earth Planet Sci Lett, 476: 153–164
Garrick-Bethell I, Seritan M R K. 2021. Laccolith Model for Lunar Ring-Moat Dome Structures. The Woodlands: 52nd Lunar and Planetary Science Conference. Abstract #2369
Gasnault O, Jeffrey Taylor G, Karunatillake S, Dohm J, Newsom H, Forni O, Pinet P, Boynton W V. 2010. Quantitative geochemical mapping of Martian elemental provinces. Icarus, 207: 226–247
Geissler P, McEwen A, Phillips C, Simonelli D, Lopes R M C, Douté S. 2001. Galileo imaging of SO_2 frosts on Io. J Geophys Res, 106: 33253–33266
Geissler P. 2015. Cryovolcanism in the outer solar system. In: Sigurdsson H, ed. The Encyclopedia of Volcanoes. New York: Academic Press. 763–776
Giardini D, Lognonné P, Banerdt W B, Pike W T, Christensen U, Ceylan S, Clinton J F, van Driel M, Stähler S C, Böse M, Garcia R F, Khan A, Panning M, Perrin C, Banfield D, Beucler E, Charalambous C, Euchner F, Horleston A, Jacob A, Kawamura T, Kedar S, Mainsant G, Scholz J R, Smrekar S E, Spiga A, Agard C, Antonangeli D, Barkaoui S, Barrett E, Combes P, Conejero V, Daubar I, Drilleau M, Ferrier C, Gabsi T, Gudkova T, Hurst K, Karakostas F, King S, Knapmeyer M, Knapmeyer-Endrun B, Llorca-Cejudo R, Lucas A, Luno L, Margerin L, McClean J B, Mimoun D, Murdoch N, Nimmo F, Nonon M, Pardo C, Rivoldini A, Manfredi J A R, Samuel H, Schimmel M, Stott A E, Stutzmann E, Teanby N, Warren T, Weber R C, Wieczorek M, Yana C. 2020. The seismicity of Mars. Nat Geosci, 13: 205–212
Glen J W. 1952. Experiments on the deformation of ice. J Glaciol, 2: 111–114
Glen J W. 1955. The creep of polycrystalline ice. Proc R Soc Lond A, 228: 519–538
Goldsby D L, Kohlstedt D L. 2001. Superplastic deformation of ice: Experimental observations. J Geophys Res-Solid Earth, 106: 11017–11030
Goudge T A, Head J W, Kerber L, Blewett D T, Denevi B W, Domingue D L, Gillis-Davis J J, Gwinner K, Helbert J, Holsclaw G M, Izenberg N R, Klima R L, McClintock W E, Murchie S L, Neumann G A, Smith D E, Strom R G, Xiao Z, Zuber M T, Solomon S C. 2014. Global inventory and characterization of pyroclastic deposits on Mercury: New insights into pyroclastic activity from MESSENGER orbital data. J Geophys Res-Planets, 119: 635–658
Grott M, Wieczorek M. 2012. Density and lithospheric structure at Tyrrhena Patera, Mars, from gravity and topography data. Icarus, 221: 43–52
Grundy W M, Binzel R P, Buratti B J, Cook J C, Cruikshank D P, Dalle Ore C M, Earle A M, Ennico K, Howett C J A, Lunsford A W, Olkin C B, Parker A H, Philippe S, Protopapa S, Quirico E, Reuter D C, Schmitt B, Singer K N, Verbiscer A J, Beyer R A, Buie M W, Cheng A F, Jennings D E, Linscott I R, Parker J W, Schenk P M, Spencer J R, Stansberry J A, Stern S A, Throop H B, Tsang C C C, Weaver H A, Weigle Ii G E, Young L A. 2016. Surface compositions across Pluto and

Charon. Science, 351: aad9189
Gülcher A J P, Gerya T V, Montési L G J, Munch J. 2020. Corona structures driven by plume–lithosphere interactions and evidence for ongoing plume activity on Venus. Nat Geosci, 13: 547–554
Halliday A N. 2000. Terrestrial accretion rates and the origin of the Moon. Earth Planet Sci Lett, 176: 17–30
Hamilton C W, Beggan C D, Still S, Beuthe M, Lopes R M C, Williams D A, Radebaugh J, Wright W. 2013. Spatial distribution of volcanoes on Io: Implications for tidal heating and magma ascent. Earth Planet Sci Lett, 361: 272–286
Hamilton C W, Fagents S A, Thordarson T. 2011. Lava-ground ice interactions in Elysium Planitia, Mars: Geomorphological and geospatial analysis of the Tartarus Colles cone groups. J Geophys Res-Planets, 116: E03004
Hansen C J, Shemansky D E, Esposito L W, Stewart A I F, Lewis B R, Colwell J E, Hendrix A R, West R A, Waite Jr. J H, Teolis B, Magee B A. 2011. The composition and structure of the Enceladus plume. Geophys Res Lett, 38: L11202
Head J W, Crumpler L S, Aubele J C, Guest J E, Saunders R S. 1992. Venus volcanism: Classification of volcanic features and structures, associations, and global distribution from Magellan data. J Geophys Res-Planets, 97: 13153–13197
Head J W, Wilson L. 1998. Tharsis Montes as composite volcanoes? 1. The role of explosive volcanism in edifice construction and implications for the volatile contents of edifice-forming magmas. Houston: 29th Lunar and Planetary Science Conference. Abstract #1127
Head J W, Wilson L. 2017. Generation, ascent and eruption of magma on the Moon: New insights into source depths, magma supply, intrusions and effusive/explosive eruptions (Part 2: Predicted emplacement processes and observations). Icarus, 283: 176–223
Hesse M A, Castillo-Rogez J C. 2019. Thermal evolution of the impact-induced cryomagma chamber beneath Occator crater on Ceres. Geophys Res Lett, 46: 1213–1221
Hiesinger H, Head J W, Wolf U, Jaumann R, Neukum G. 2011. Ages and stratigraphy of lunar mare basalts: A synthesis. In: Ambrose W A, Williams D A, eds. Recent Advances and Current Research Issues in Lunar Stratigraphy. Special Paper of the Geological Society of America. 477: 1–51
Horvath D G, Moitra P, Hamilton C W, Craddock R A, Andrews-Hanna J C. 2021. Evidence for geologically recent explosive volcanism in Elysium Planitia, Mars. Icarus, 365: 114499
Hu S, He H, Ji J, Lin Y, Hui H, Anand M, Tartèse R, Yan Y, Hao J, Li R, Gu L, Guo Q, He H, Ouyang Z. 2021. A dry lunar mantle reservoir for young mare basalts of Chang'e-5. Nature, 600: 49–53
Huang J, Xiao L. 2014. Knobby terrain on ancient volcanoes as an indication of dominant early explosive volcanism on Mars. Geophys Res Lett, 41: 7019–7024
Ivanov M A, Crumpler L S, Aubele J C, Head J W. 2015. Volcanism on Venus. In: Sigurdsson H, ed. The Encyclopedia of Volcanoes. New York: Academic Press. 729–746
Ivanov M A, Hiesinger H, Erkeling G, Reiss D. 2014. Mud volcanism and morphology of impact craters in Utopia Planitia on Mars: Evidence for the ancient ocean. Icarus, 228: 121–140
Johnson T V, Veeder G J, Matson D L, Brown R H, Nelson R M, Morrison D. 1988. Io: Evidence for silicate volcanism in 1986. Science, 242: 1280–1283
Jolliff B L, Gillis J J, Haskin L A, Korotev R L, Wieczorek M A. 2000. Major lunar crustal terranes: Surface expressions and crust-mantle origins. J Geophys Res, 105: 4197–4216
Jozwiak L M, Head J W, Wilson L. 2018. Explosive volcanism on Mercury: Analysis of vent and deposit morphology and modes of eruption. Icarus, 302: 191–212
Kamata S, Nimmo F, Sekine Y, Kuramoto K, Noguchi N, Kimura J, Tani A. 2019. Pluto's ocean is capped and insulated by gas hydrates. Nat Geosci, 12: 407–410
Kargel J S. 1991. Brine volcanism and the interior structures of asteroids and icy satellites. Icarus, 94: 368–390
Kargel J S. 1995. Cryovolcanism on the icy satellites. In: Chahine M T, A'Hearn M F, Rahe J, eds. Comparative Planetology with an Earth Perspective. Dordrecht: Springer. 101–113
Kargel J S, Pozio S. 1996. The volcanic and tectonic history of Enceladus. Icarus, 119: 385–404
Keane J T, de Kleer K, Rathbun J, Ahern A, Radebaugh J. 2018. Comprehensive spherical harmonic analysis of the distribution of Io's volcanoes, mountains, heat flow, and other geologic phenomena. Washington DC: 2018 AGU Fall Meeting. P53C-2983
Kerber L, Head J W, Solomon S C, Murchie S L, Blewett D T, Wilson L. 2009. Explosive volcanic eruptions on Mercury: Eruption conditions, magma volatile content, and implications for interior volatile abundances. Earth Planet Sci Lett, 285: 263–271
Keszthelyi L, McEwen A S, Phillips C B, Milazzo M, Geissler P, Turtle E P, Radebaugh J, Williams D A, Simonelli D P, Breneman H H, Klaasen K P, Levanas G, Denk T. 2001. Imaging of volcanic activity on Jupiter's moon Io by Galileo during the Galileo Europa Mission and the Galileo Millennium Mission. J Geophys Res-Planets, 106: 33025–33052
Khurana K K, Kivelson M G, Stevenson D J, Schubert G, Russell C T, Walker R J, Polanskey C. 1998. Induced magnetic fields as evidence for subsurface oceans in Europa and Callisto. Nature, 395: 777–780
Kivelson M G, Khurana K K, Russell C T, Volwerk M, Walker R J, Zimmer C. 2000. Galileo magnetometer measurements: A stronger case for a subsurface ocean at Europa. Science, 289: 1340–1343
Kleine T, Münker C, Mezger K, Palme H. 2002. Rapid accretion and early core formation on asteroids and the terrestrial planets from Hf–W chronometry. Nature, 418: 952–955
Laneuville M, Wieczorek M A, Breuer D, Tosi N. 2013. Asymmetric thermal evolution of the Moon. J Geophys Res-Planets, 118: 1435–1452
Laver C, de Pater I. 2009. The global distribution of sulfur dioxide ice on Io, observed with OSIRIS on the W.M. Keck telescope. Icarus, 201: 172–181
Li Q L, Zhou Q, Liu Y, Xiao Z, Lin Y, Li J H, Ma H X, Tang G Q, Guo S, Tang X, Yuan J Y, Li J, Wu F Y, Ouyang Z, Li C, Li X H. 2021. Two-billion-year-old volcanism on the Moon from Chang'e-5 basalts. Nature, 600: 54–58
Linde A T, Sacks I S. 1998. Triggering of volcanic eruptions. Nature, 395: 888–890
Liu S, Zhou Q, Li Q, Hu S, Yang W. 2021. Chang'e-5 samples reveal two-billion-year-old volcanic activity on the Moon and its source characteristics. Sci China Earth Sci, 64: 2083–2089
Lucchitta B K, Soderblom L A. 1982. The geology of Europa. In: Satellites of Jupiter. Tucson: University of Arizona Press. 521–555
Lunine J I, Stevenson D J. 1985. Thermodynamics of clathrate hydrate at low and high pressures with application to the outer solar system. Astrophys J Suppl Ser, 58: 493–531
Mancinelli P, Minelli F, Pauselli C, Federico C. 2016. Geology of the Raditladi quadrangle, Mercury (H04). J Maps, 12: 190–202
Marchi S, Chapman C R, Fassett C I, Head J W, Bottke W F, Strom R G. 2013. Global resurfacing of Mercury 4.0–4.1 billion years ago by heavy bombardment and volcanism. Nature, 499: 59–61
Marcq E, Bertaux J L, Montmessin F, Belyaev D. 2013. Variations of sulphur dioxide at the cloud top of Venus's dynamic atmosphere. Nat Geosci, 6: 25–28
McCoy T J, Peplowski P N, McCubbin F M, Weider S Z. 2018. The geochemical and mineralogical diversity of Mercury. In: Solomon S C, Nittler L R, Anderson B J, eds. Mercury: The View After MESSENGER. Cambridge: Cambridge Planetary Science. 176–190
McEwen A S, Malin M C, Carr M H, Hartmann W K. 1999. Voluminous volcanism on early Mars revealed in Valles Marineris. Nature, 397: 584–586
McEwen A S, Keszthelyi L, Spencer J R, Schubert G, Matson D L, Lopes-Gautier R, Klaasen K P, Johnson T V, Head J W, Geissler P, Fagents S, Davies A G, Carr M H, Breneman H H, Belton M J S. 1998. High-temperature silicate volcanism on Jupiter's Moon Io. Science, 281: 87–90
McKinnon W B, Stern S A, Weaver H A, Nimmo F, Bierson C J, Grundy W M, Cook J C, Cruikshank D P, Parker A H, Moore J M, Spencer J R,

Young L A, Olkin C B, Ennico Smith K, New Horizons Geology G. 2017. Origin of the Pluto-Charon system: Constraints from the New Horizons flyby. Icarus, 287: 2–11
McLennan S M, Anderson R B, Bell III J F, Bridges J C, Calef III F, Campbell J L, Clark B C, Clegg S, Conrad P, Cousin A, et al., a total of 448 authors. 2014. Elemental geochemistry of sedimentary rocks at Yellowknife Bay, Gale crater, Mars. Science, 343: 1244734
Michalski J R, Bleacher J E. 2013. Supervolcanoes within an ancient volcanic province in Arabia Terra, Mars. Nature, 502: 47–52
Milazzo M P, Keszthelyi L P, Radebaugh J, Davies A G, Turtle E P, Geissler P, Klaasen K P, Rathbun J A, McEwen A S. 2005. Volcanic activity at Tvashtar Catena, Io. Icarus, 179: 235–251
Mitchell R N. 2021. Chang'E-5 reveals the Moon's secrets to a longer life. Innovation, 2: 100177
Moore J M, McKinnon W B, Spencer J R, Howard A D, Schenk P M, Beyer R A, Nimmo F, Singer K N, Umurhan O M, White O L, et al., a total of 154 authors. 2016. The geology of Pluto and Charon through the eyes of New Horizons. Science, 351: 1284–1293
Murchie S L, Klima R L, Izenberg N R, Domingue D L, Blewett D T, Helbert J. 2018. Spectral reflectance Constraints on the Composition and Evolution of Mercury's Surface. In: Solomon S C, Nittler L R, Anderson B J, eds. Mercury: The View After MESSENGER. Cambridge: Cambridge Planetary Science. 191–216
Nimmo F, McKenzie D. 1998. Volcanism and tectonics on Venus. Annu Rev Earth Planet Sci, 26: 23–51
Ody A, Poulet F, Langevin Y, Bibring J P, Bellucci G, Altieri F, Gondet B, Vincendon M, Carter J, Manaud N. 2012. Global maps of anhydrous minerals at the surface of Mars from OMEGA/Mex. J Geophys Res, 117: E00J14
Padovan S, Tosi N, Plesa A C, Ruedas T. 2017. Impact-induced changes in source depth and volume of magmatism on Mercury and their observational signatures. Nat Commun, 8: 1945
Peplowski P N, Klima R L, Lawrence D J, Ernst C M, Denevi B W, Frank E A, Goldsten J O, Murchie S L, Nittler L R, Solomon S C. 2016. Remote sensing evidence for an ancient carbon-bearing crust on Mercury. Nat Geosci, 9: 273–276
Plescia J B. 2004. Morphometric properties of Martian volcanoes. J Geophys Res, 109: E03003
Qi C, Stern L A, Pathare A, Durham W B, Goldsby D L. 2018. Inhibition of grain boundary sliding in fine-grained ice by intergranular particles: Implications for planetary ice masses. Geophys Res Lett, 45: 12,757–12,765
Qian Y, She Z, He Q, Xiao L, Wang Z, Head J W, Sun L, Wang Y, Wu B, Wu X, Luo B, Cao K, Li Y, Dong M, Song W, Pan F, Michalski J, Ye B, Zhao J, Zhao S, Huang J, Zhao J, Wang J, Zong K, Hu Z. 2023. Mineralogy and chronology of the young mare volcanism in the Procellarum-KREEP-Terrane. Nat Astron, 7: 287–297
Qian Y, Xiao L, Wang Q, Head J W, Yang R, Kang Y, van der Bogert C H, Hiesinger H, Lai X, Wang G, Pang Y, Zhang N, Yuan Y, He Q, Huang J, Zhao J, Wang J, Zhao S. 2021. China's Chang'e-5 landing site: Geology, stratigraphy, and provenance of materials. Earth Planet Sci Lett, 561: 116855
Qiao L, Chen J, Ling Z. 2021. Volcanic landforms on the Moon (in Chinese). Acta Geol Sin, 95: 2678–2691
Qiao L, Head J W, Ling Z, Wilson L. 2020. Lunar irregular mare patches: Classification, characteristics, geologic settings, updated catalog, origin, and outstanding questions. J Geophys Res-Planets, 125: e06362
Qiao L, Head J, Wilson L, Xiao L, Kreslavsky M, Dufek J. 2017. Ina pit crater on the Moon: Extrusion of waning-stage lava lake magmatic foam results in extremely young crater retention ages. Geology, 45: 455–458
Quick L C, Buczkowski D L, Ruesch O, Scully J E C, Castillo-Rogez J, Raymond C A, Schenk P M, Sizemore H G, Sykes M V. 2019. A possible brine reservoir beneath Occator crater: Thermal and compositional evolution and formation of the Cerealia dome and Vinalia Faculae. Icarus, 320: 119–135
Quick L C, Glaze L S, Baloga S M. 2017. Cryovolcanic emplacement of domes on Europa. Icarus, 284: 477–488
Raymond C A, Ermakov A I, Castillo-Rogez J C, Marchi S, Johnson B C, Hesse M A, Scully J E C, Buczkowski D L, Sizemore H G, Schenk P M, Nathues A, Park R S, Prettyman T H, Quick L C, Keane J T, Rayman M D, Russell C T. 2020. Impact-driven mobilization of deep crustal brines on dwarf planet Ceres. Nat Astron, 4: 741–747
Robbins S J, di Achille G, Hynek B M. 2011. The volcanic history of Mars: High-resolution crater-based studies of the calderas of 20 volcanoes. Icarus, 211: 1179–1203
Rogers A D, Christensen P R. 2007. Surface mineralogy of Martian low-albedo regions from MGS-TES data: Implications for upper crustal evolution and surface alteration. J Geophys Res-Planets, 112: E01003
Rogers A D, Nazarian A H. 2013. Evidence for Noachian flood volcanism in Noachis Terra, Mars, and the possible role of Hellas impact basin tectonics. J Geophys Res-Planets, 118: 1094–1113
Roth L, Saur J, Retherford K D, Strobel D F, Feldman P D, McGrath M A, Nimmo F. 2014. Transient water vapor at Europa's south pole. Science, 343: 171–174
Ruesch O, Genova A, Neumann W, Quick L C, Castillo-Rogez J C, Raymond C A, Russell C T, Zuber M T. 2019. Slurry extrusion on Ceres from a convective mud-bearing mantle. Nat Geosci, 12: 505–509
Ruesch O, Platz T, Schenk P, McFadden L A, Castillo-Rogez J C, Quick L C, Byrne S, Preusker F, O'Brien D P, Schmedemann N, Williams D A, Li J Y, Bland M T, Hiesinger H, Kneissl T, Neesemann A, Schaefer M, Pasckert J H, Schmidt B E, Buczkowski D L, Sykes M V, Nathues A, Roatsch T, Hoffmann M, Raymond C A, Russell C T. 2016. Cryovolcanism on ceres. Science, 353: aaf4286
Salvatore M R, Christensen P R. 2014. On the origin of the Vastitas Borealis formation in Chryse and Acidalia Planitiae, Mars. J Geophys Res-Planets, 119: 2437–2456
Schenk P M, McKinnon W B, Gwynn D, Moore J M. 2001. Flooding of Ganymede's bright terrains by low-viscosity water-ice lavas. Nature, 410: 57–60
Sehlke A, Whittington A G. 2015. Rheology of lava flows on Mercury: An analog experimental study. J Geophys Res-Planets, 120: 1924–1955
Singer K N, White O L, Schmitt B, Rader E L, Protopapa S, Grundy W M, Cruikshank D P, Bertrand T, Schenk P M, McKinnon W B, Stern S A, Dhingra R D, Runyon K D, Beyer R A, Bray V J, Ore C D, Spencer J R, Moore J M, Nimmo F, Keane J T, Young L A, Olkin C B, Lauer T R, Weaver H A, Ennico-Smith K. 2022. Large-scale cryovolcanic resurfacing on Pluto. Nat Commun, 13: 1542
Smrekar S E, Stofan E R, Mueller N, Treiman A, Elkins-Tanton L, Helbert J, Piccioni G, Drossart P. 2010. Recent hotspot volcanism on Venus from VIRTIS emissivity data. Science, 328: 605–608
Solomon S C, Ahrens T J, Reynolds R T, Cassen P M, Sleep N H, Minerar J W, Turcotte D L. 1981. Thermal histories of the terrerstrail planets. In: Basaltic Volcanism on the Therrestrial Planets. Basaltic Volcanism Study Project. New York: Pergamon Press. 1130–1237
Sori M M, Byrne S, Bland M T, Bramson A M, Ermakov A I, Hamilton C W, Otto K A, Ruesch O, Russell C T. 2017. The vanishing cryovolcanoes of Ceres. Geophys Res Lett, 44: 1243–1250
Sori M M, Sizemore H G, Byrne S, Bramson A M, Bland M T, Stein N T, Russell C T. 2018. Cryovolcanic rates on Ceres revealed by topography. Nat Astron, 2: 946–950
Sparks W B, Hand K P, McGrath M A, Bergeron E, Cracraft M, Deustua S E. 2016. Probing for evidence of plumes on europa with *HST*/STIS. Astrophys J, 829: 121
Sparks W B, Schmidt B E, McGrath M A, Hand K P, Spencer J R, Cracraft M, Deustua S E. 2017. Active cryovolcanism on Europa? Astrophys J, 839: L18
Spudis P D, Guest J E. 1988. Stratigraphy and geologic history of Mercury. In: Vilas F, Chapman C R, Matthews M S, eds. Mercury. Tucson: University of Arizona Press. 118–164
Squyres S W, Reynolds R T, Cassen P M, Peale S J. 1983. Liquid water and active resurfacing on Europa. Nature, 301: 225–226
Stockstill-Cahill K R, McCoy T J, Nittler L R, Weider S Z, Hauck Steven A. I I. 2012. Magnesium-rich crustal compositions on Mercury: Implications for magmatism from petrologic modeling. J Geophys Res, 117: E00L15

Stofan E R, Sharpton V L, Schubert G, Baer G, Bindschadler D L, Janes D M, Squyres S W. 1992. Global distribution and characteristics of coronae and related features on Venus: Implications for origin and relation to mantle processes. J Geophys Res-Planets, 97: 13347–13378
Strom R G, Banks M E, Chapman C R, Fassett C I, Forde J A, Head Iii J W, Merline W J, Prockter L M, Solomon S C. 2011. Mercury crater statistics from MESSENGER flybys: Implications for stratigraphy and resurfacing history. Planet Space Sci, 59: 1960–1967
Strom R G, Schaber G G, Dawsow D D. 1994. The global resurfacing of Venus. J Geophys Res-Planets, 99: 10899–10926
Tanaka K L, Skinner J A, Dohm J M, Irwin III R P, Kolb E J, Fortezzo C M, Platz T, Hare T M. 2014. Geologic Map of Mars. Flagstaff: United States Geological Survey
Tartèse R, Anand M, Gattacceca J, Joy K H, Mortimer J I, Pernet-Fisher J F, Russell S, Snape J F, Weiss B P. 2019. Constraining the evolutionary history of the Moon and the Inner Solar System: A case for new returned lunar samples. Space Sci Rev, 215: 54
Terada K, Anand M, Sokol A K, Bischoff A, Sano Y. 2007. Cryptomare magmatism 4.35 Gyr ago recorded in lunar meteorite Kalahari 009. Nature, 450: 849–852
Thomas R J, Rothery D A, Conway S J, Anand M. 2014. Long-lived explosive volcanism on Mercury. Geophys Res Lett, 41: 6084–6092
Thomas R J, Rothery D A, Conway S J, Anand M. 2015. Explosive volcanism in complex impact craters on Mercury and the Moon: Influence of tectonic regime on depth of magmatic intrusion. Earth Planet Sci Lett, 431: 164–172
Tian H C, Wang H, Chen Y, Yang W, Zhou Q, Zhang C, Lin H L, Huang C, Wu S T, Jia L H, Xu L, Zhang D, Li X G, Chang R, Yang Y H, Xie L W, Zhang D P, Zhang G L, Yang S H, Wu F Y. 2021. Non-KREEP origin for Chang'e-5 basalts in the Procellarum KREEP Terrane. Nature, 600: 59–63
Trask N J, Guest J E. 1975. Preliminary geologic terrain map of Mercury. J Geophys Res, 80: 2461–2477
Travis B J, Bland P A, Feldman W C, Sykes M V. 2018. Hydrothermal dynamics in a CM-based model of Ceres. Meteorit Planet Sci, 53: 2008–2032
Tyler R H, Henning W G, Hamilton C W. 2015. Tidal heating in a magma ocean within Jupiter's moon Io. Astrophys J Suppl Ser, 218: 22
Vander Kaaden K E, McCubbin F M, Nittler L R, Peplowski P N, Weider S Z, Frank E A, McCoy T J. 2017. Geochemistry, mineralogy, and petrology of boninitic and komatiitic rocks on the mercurian surface: Insights into the mercurian mantle. Icarus, 285: 155–168
Vaniman D T, Bish D L, Ming D W, Bristow T F, Morris R V, Blake D F, Chipera S J, Morrison S M, Treiman A H, Rampe E B, Rice M, Achilles C N, Grotzinger J P, McLennan S M, Williams J, Bell III J F, Newsom H E, Downs R T, Maurice S, Sarrazin P, Yen A S, Morookian J M, Farmer J D, Stack K, Milliken R E, Ehlmann B L, Sumner D Y, Berger G, Crisp J A, Hurowitz J A, Anderson R, Des Marais D J, Stolper E M, Edgett K S, Gupta S, Spanovich N, the MSL Science Team. 2014. Mineralogy of a mudstone at Yellowknife Bay, Gale crater, Mars. Science, 343: 1243480
Veeder G J, Davies A G, Matson D L, Johnson T V, Williams D A, Radebaugh J. 2012. Io: Volcanic thermal sources and global heat flow. Icarus, 219: 701–722
Veeder G J, Davies A G, Matson D L, Johnson T V, Williams D A, Radebaugh J. 2015. Io: Heat flow from small volcanic features. Icarus, 245: 379–410
Veeder G J, Matson D L, Johnson T V, Blaney D L, Goguen J D. 1994. Io's heat flow from infrared radiometry: 1983–1993. J Geophys Res, 99: 17095–17162
Waite J H, Glein C R, Perryman R S, Teolis B D, Magee B A, Miller G, Grimes J, Perry M E, Miller K E, Bouquet A, Lunine J I, Brockwell T, Bolton S J. 2017. Cassini finds molecular hydrogen in the Enceladus plume: Evidence for hydrothermal processes. Science, 356: 155–159
Wang Y C, Xiao Z Y, Chang Y R, Xu R, Cui J. 2021. Short-term and global-wide effusive volcanism on Mercury around 3.7 Ga. Geophys Res Lett, 48: e2021GL094503
Warren P H. 1985. The magma ocean concept and lunar evolution. Annu Rev Earth Planet Sci, 13: 201–240
Weider S Z, Nittler L R, Murchie S L, Peplowski P N, McCoy T J, Kerber L, Klimczak C, Ernst C M, Goudge T A, Starr R D, Izenberg N R, Klima R L, Solomon S C. 2016. Evidence from MESSENGER for sulfur- and carbon-driven explosive volcanism on Mercury. Geophys Res Lett, 43: 3653–3661
Werner S C. 2009. The global martian volcanic evolutionary history. Icarus, 201: 44–68
Whitten J L, Head J W, Denevi B W, Solomon S C. 2014. Intercrater plains on Mercury: Insights into unit definition, characterization, and origin from MESSENGER datasets. Icarus, 241: 97–113
Whitten J L, Head J W. 2015a. Lunar cryptomaria: Physical characteristics, distribution, and implications for ancient volcanism. Icarus, 247: 150–171
Whitten J L, Head J W. 2015b. Rembrandt impact basin: Distinguishing between volcanic and impact-produced plains on Mercury. Icarus, 258: 350–365
Wilson L. 2009. Volcanism in the Solar System. Nat Geosci, 2: 389–397
Wilson L, Head III J W. 1981. Ascent and eruption of basaltic magma on the Earth and Moon. J Geophys Res-Solid Earth, 86: 2971–3001
Wilson L, Head J W, Zhang F. 2019. A theoretical model for the formation of Ring Moat Dome Structures: Products of second boiling in lunar basaltic lava flows. J Volcanol Geotherm Res, 374: 160–180
Wray J J, Hansen S T, Dufek J, Swayze G A, Murchie S L, Seelos F P, Skok J R, Irwin Iii R P, Ghiorso M S. 2013. Prolonged magmatic activity on Mars inferred from the detection of felsic rocks. Nat Geosci, 6: 1013–1017
Xiao L, Greeley R. 2008. Characteristics of volcanism and evolution of Mars (in Chinese). Bull Mineral Petrol Geochem, 27: 60–61
Xiao L, Huang J, Christensen P R, Greeley R, Williams D A, Zhao J, He Q. 2012. Ancient volcanism and its implication for thermal evolution of Mars. Earth Planet Sci Lett, 323-324: 9–18
Xiao L. 2013. Planetary Geology (in Chinese). Beijing: Geology Press. 495
Xiao Z Y, Xu R, Wang Y C, Chang Y R, Xu R, Cui J. 2021. Recent dark pyroclastic deposits on Mercury. Geophys Res Lett, 48: e92532
Ye B, Qian Y, Xiao L, Michalski J R, Li Y, Wu B, Qiao L. 2021. Geomorphologic exploration targets at the Zhurong landing site in the southern Utopia Planitia of Mars. Earth Planet Sci Lett, 576: 117199
Yin Q, Jacobsen S B, Yamashita K, Blichert-Toft J, Télouk P, Albarède F. 2002. A short timescale for terrestrial planet formation from Hf-W chronometry of meteorites. Nature, 418: 949–952
Zhang F, Head J W, Wöhler C, Basilevsky A T, Wilson L, Xie M, Bugiolacchi R, Wilhelm T, Althoff S, Zou Y L. 2021. The Lunar Mare Ring-Moat Dome Structure (RMDS) age conundrum: Contemporaneous with imbrian-aged host lava flows or emplaced in the Copernican? J Geophys Res-Planets, 126: e06880
Zhang F, Head J W, Wöhler C, Bugiolacchi R, Wilson L, Basilevsky A T, Grumpe A, Zou Y L. 2020. Ring-Moat Dome Structures (RMDSs) in the Lunar Maria: Statistical, compositional, and morphological characterization and assessment of theories of origin. J Geophys Res-Planets, 125: e05967
Zhang F, Head J W, Basilevsky A T, Bugiolacchi R, Komatsu G, Wilson L, Fa W, Zhu M H. 2017. Newly discovered ring-moat dome structures in the Lunar Maria: Possible origins and implications. Geophys Res Lett, 44: 9216–9224
Zhao J, Xiao Z, Huang J, Head J W, Wang J, Shi Y, Wu B, Wang L. 2021. Geological characteristics and targets of high scientific interest in the Zhurong landing region on Mars. Geophys Res Lett, 48: e94903
Zhou C, Jia Y, Liu J, Li H, Fan Y, Zhang Z, Liu Y, Jiang Y, Zhou B, He Z, Yang J, Hu Y, Liu Z, Qin L, Lv B, Fu Z, Yan J, Wang C, Zou Y. 2022. Scientific objectives and payloads of the lunar sample return mission—Chang'E-5. Adv Space Res, 69: 823–836

(Editorial handling: Hejiu HUI)